LANGTRY, TINA M.--CARBONATE BODIES WITHIN THE BASAL SWIFT FORMATION (JURASSIC) OF NORTHWESTERN NORTH DAKOTA
North Dakota Geological Survey R.I. No. 81

CARBONATE BODIES WITHIN THE BASAL SWIFT FORMATION (JURASSIC) OF NORTHWESTERN NORTH DAKOTA

by

Tina M. Langtry

REPORT OF INVESTIGATION NO. 81

NORTH DAKOTA GEOLOGICAL SURVEY

Don L. Halvorson, State Geologist

1983

CARBONATE BODIES WITHIN THE BASAL SWIFT FORMATION (JURASSIC) OF NORTHWESTERN NORTH DAKOTA

by

Tina M. Langtry

REPORT OF INVESTIGATION NO. 81

NORTH DAKOTA GEOLOGICAL SURVEY

Don L. Halvorson, State Geologist

1983

Printed by Richtman's-Midwest Printing - Fargo, North Dakota 58102

CONTENTS

ILLUSTRATIONS

ABSTRACT

The carbonate bodies of the basal Swift Formation (Upper Jurassic) occur as anomalous deflections on a relatively uniform mechanical well-log section. The areal distribution, stratigraphic relationships, and genesis of the carbonate bodies were determined using the gamma-ray log, the spontaneous-potential log, the resistivity log suite, and megascopic and microscopic core analysis.

The carbonate bodies of the basal Swift Formation were found to be coarsening-upward sequences composed of predominantly sand-sized, recrystallized mollusk grains. These grains were transported by strong bottom currents across the irregular sea floor of the shallow epicontinental Jurassic sea, and were deposited under agitated water conditions in the offshore environment. These carbonate sand bodies are analogous to offshore-bar deposits of similar age that are recognized across the midcontinent region.

The carbonate sand bodies are up to 22 miles long and 7 miles wide, and as thick as 155 feet. The bioclastic sand bodies have a lower contact that is apparently gradational with the underlying very fine grained quartzarenites. The base of the carbonate body is composed of a finely laminated, recrystallized molluscan packstone that has a low porosity and contains moderate amounts of siliciclastic material in the matrix. This recrystallized molluscan packstone becomes cleaner and coarsens upward into a massive (?), recrystallized molluscan grainstone with high moldic porosity and good permeability.

The shape of the carbonate bodies, their high moldic porosity and good permeability of the grainstones, coupled with the seal provided by the overlying shale, makes these basal Swift carbonate bodies good reservoir rocks. The shallow depth of burial and the thermal immaturity of the surrounding shales makes it unlikely that thermally generated hydrocarbons will be found in the carbonate bodies. However, the possibility of the existence of biogenic gas, derived from the surrounding shales, makes these deposits potential sites for exploration.

INTRODUCTION

Purpose

The purpose of this study has been to critically examine the Swift Formation carbonate bodies. In doing so, the author has mapped the location of the bodies recognized within the study area, attempted to stratigraphically define the bodies within the Swift Formation, to define the nature of the contacts between the carbonate bodies and the surrounding Swift Formation, and to determine the genesis of the carbonate bodies.

Area of Study

The Williston Basin is an irregularly shaped intracratonic basin located in the center of the North American continent between the Canadian Shield and the Rocky Mountains. The basin occupies portions of Manitoba, Saskatchewan, Montana, South Dakota, and North Dakota (fig. 1).

Initial subsurface work located 53 apparently similar bodies widely scattered across the western half of North Dakota (fig. 2). Because of the detailed nature of this study, examination of the carbonate bodies was limited to the area outlined in figure 3. This area was chosen for its known concentration of carbonate bodies.

Regional Setting

The deposition of the Jurassic sediments within the northern Rocky Mountains and the Williston Basin was predominantly a function of several transgressive-regressive cycles of a marine interior sea, which extended from northwestern Canada southward into the northern Rocky Mountain region. No marine rocks of the Lower Jurassic have been recognized south of the Alberta Trough. Significant deposition probably did not occur in the Williston Basin until Middle Jurassic time (Peterson, 1958).

Several paleotectonic features were active during the Middle and Late Jurassic within the Williston Basin region (fig. 4). The Belt Island probably exerted the most influence on the distribution of marine currents, temperatures, salinities, and sedimentation within the basin up until Swift (Oxfordian) time (Peterson, 1957).

Deposition of the Swift Formation took place during the final transgressive-regressive cycle of the marine Jurassic seas and shortly after the initiation of the Nevadian Orogeny in western Montana, eastern Idaho, and western Utah. The presence of an active clastic source to the west and the decline in the influence of the Belt Island and the Sheridan Arch, coupled with the erosion of the Precambrian Shield, caused clastic deposition to be dominant within the basin area. At that time, the basin depocenter was located near the Montana-North Dakota border (Carlson, 1968).

General Stratigraphy

The Rierdon Formation conformably underlies the Swift Formation throughout the study area. It consists of varicolored shades of gray, green, and red calcareous shales. Some limestones are also present (Bluemle, Anderson, and Carlson, 1980). The maximum thickness of the Rierdon within North Dakota is 100 feet.

The Swift Formation is predominantly a transgressive-regressive, clastic, shallow marine deposit composed of dark-gray to greenish shales, and slightly calcareous, glauconitic siltstones and sandstones. Thickness within the study area ranges from 264 feet in the northeastern corner to 497 feet in the southwestern corner (pl. 1). Localized limestones have also been noted (Milnor and Thomas, 1954; Bluemle, Anderson, and Carlson, 1980).

The basal 150 to 200 feet of the Swift Formation are predominantly beds of slightly calcareous, dark-gray to greenish, waxy shales. These shales are commonly interbedded with glauconitic siltstones and sandstones. Locally, carbonate units consisting of sand-sized skeletal packstones and grainstones are present. The carbonate units range from a few feet to 155 feet thick within the study area (pl. 2). The upper half of the Swift consists of shaly, glauconitic siltstones and sandstones with associated shales (Bluemle, Anderson, and Carlson, 1980).

The Lower Cretaceous Inyan Kara Formation unconformably overlies the Swift Formation within the study area. The lower Inyan Kara is a non-marine, medium- to coarse-grained, quartzose sandstone. Occasionally, lenses of bentonitic shale are also present. The upper Inyan Kara is a transitional

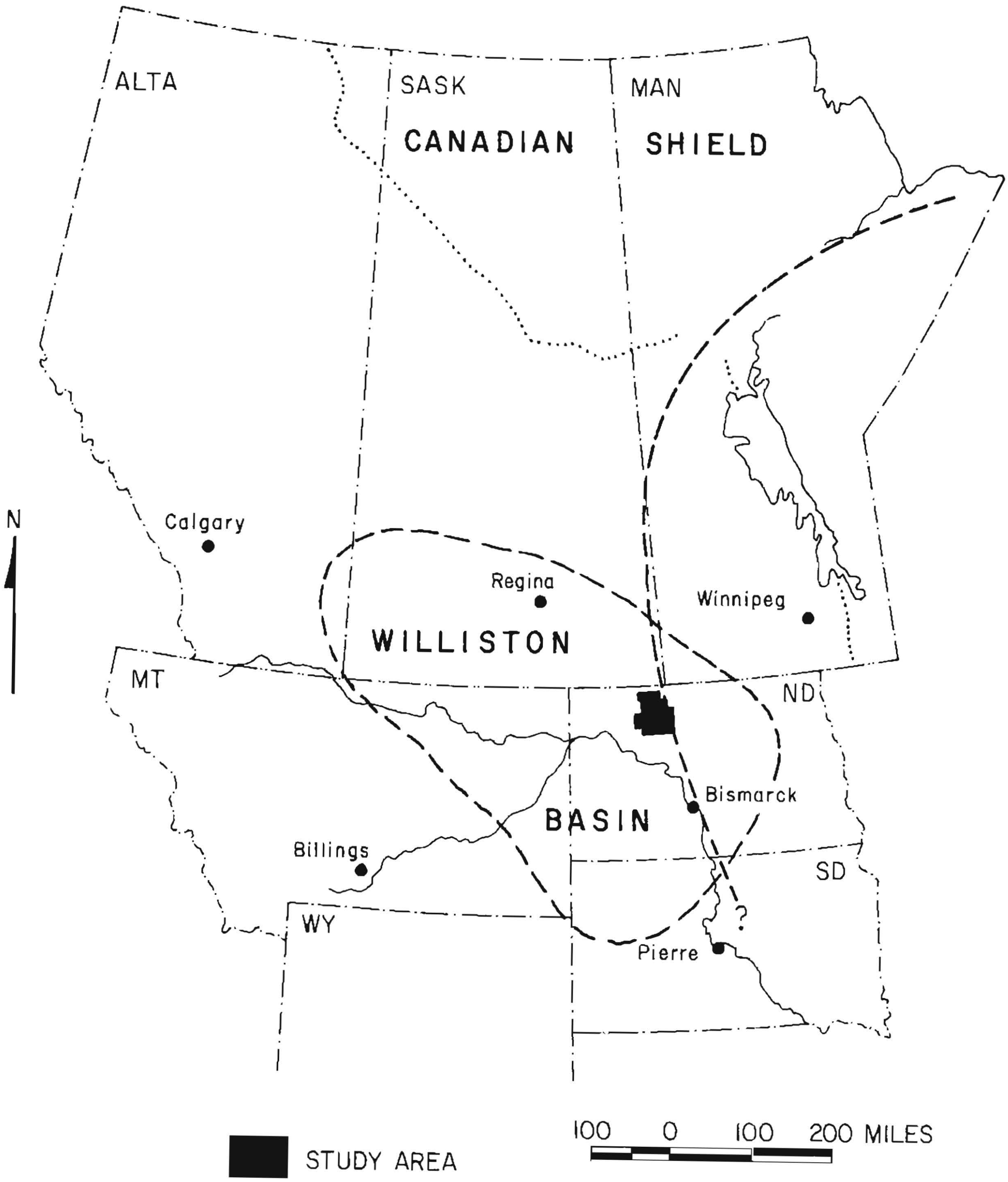

Figure 1. Williston Basin location map.

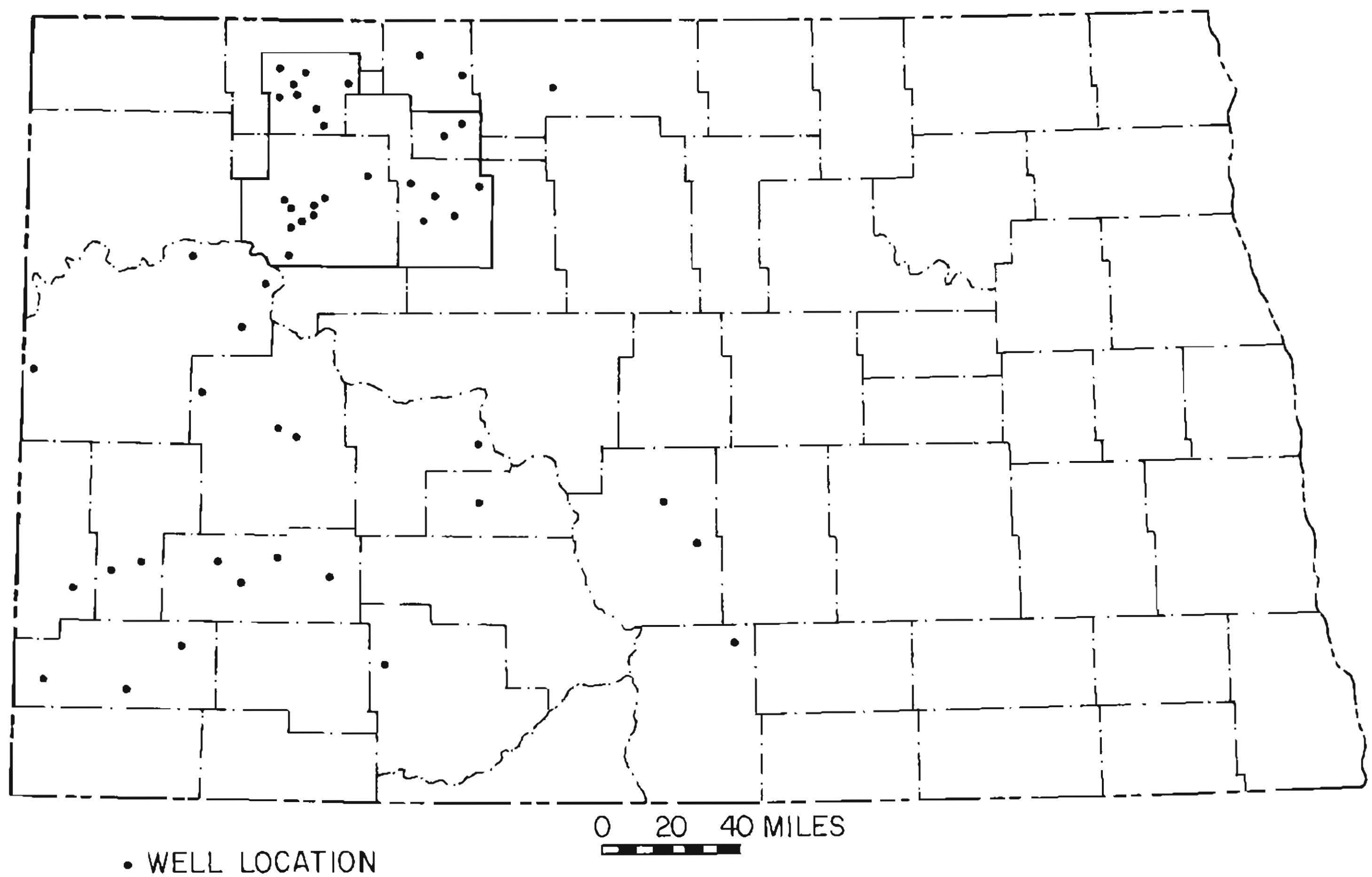

Figure 2. Location map of the carbonate bodies within the basal Swift Formation, initially recognized within the North Dakota portion of the Williston Basin.

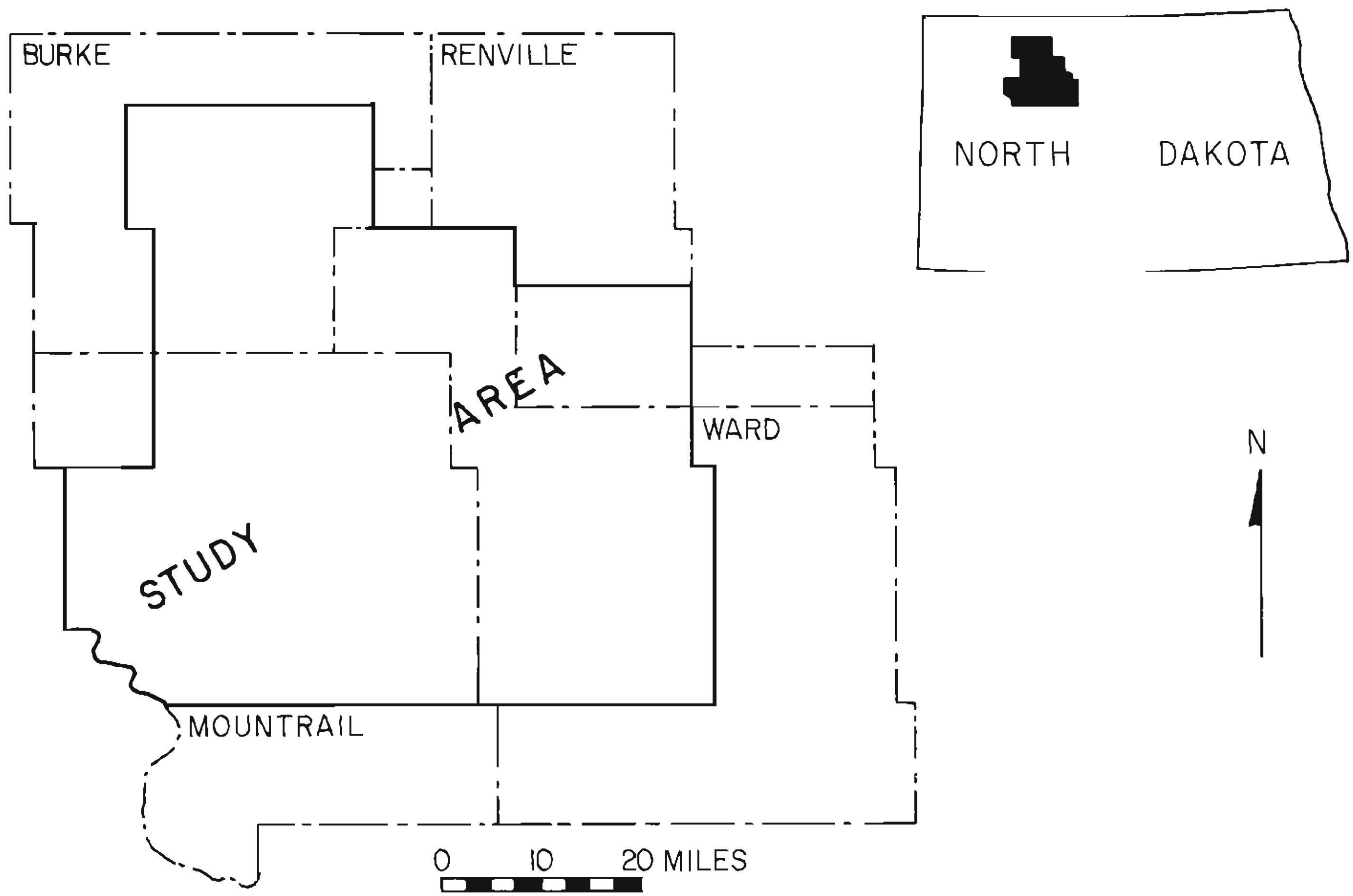

Figure 3. Location of the area of study within North Dakota.

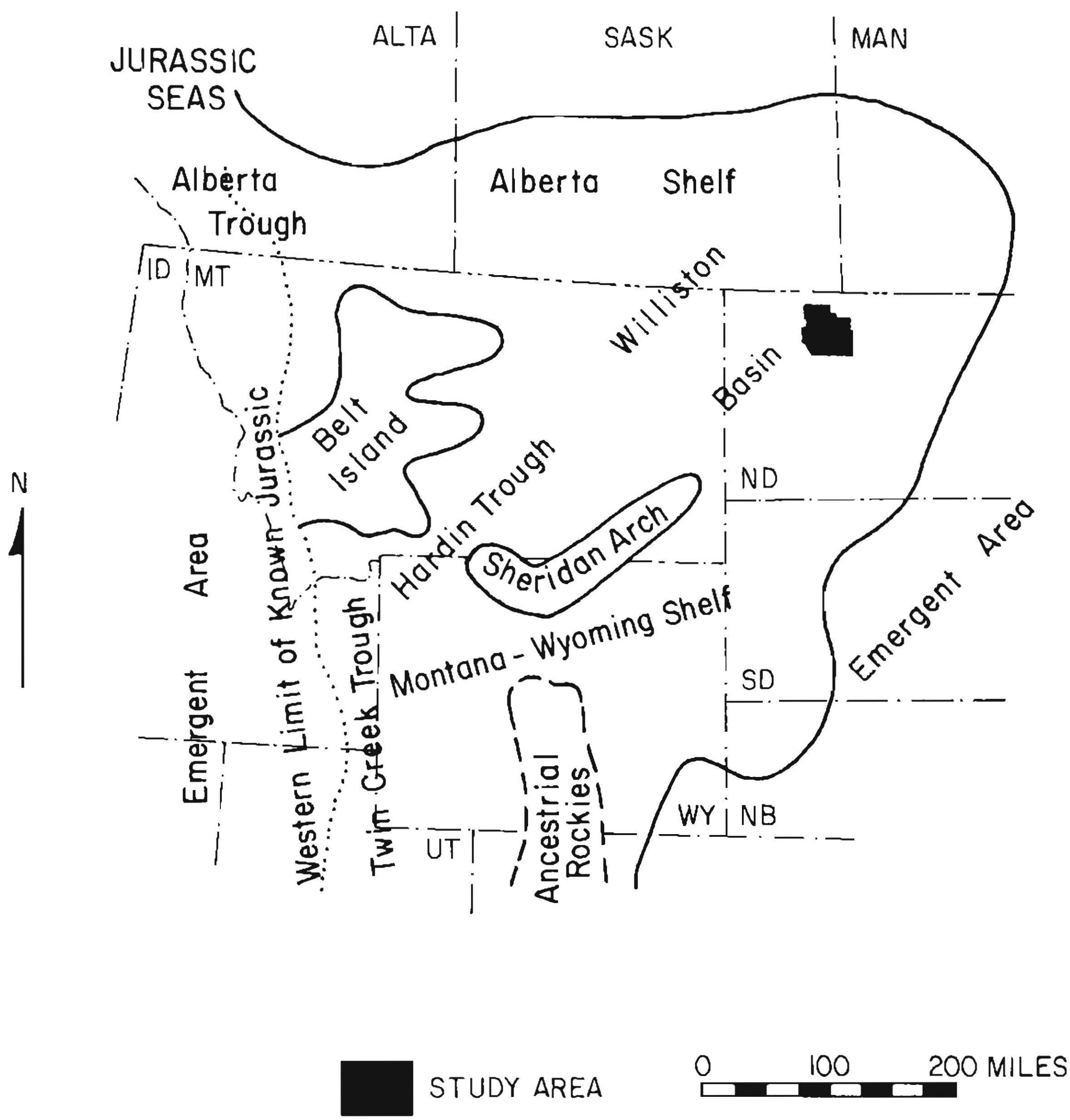

Figure 4. Map of the paleotectonic features active during the Middle and Late Jurassic within the Williston Basin region (after Peterson, 1957, p. 403).

marine, light-gray, fine- to coarse-grained, quartzose sandstone with interbedded shales (Bluemle, Anderson, and Carlson, 1980). The maximum thickness of the Inyan Kara Formation within the state is 450 feet.

The North Dakota Geological Survey is formally using the Piper, Rierdon, and Swift Formations (Bluemle, Anderson, and Carlson, 1981) (table 1). No rocks equivalent to the Morrison Formation are recognized within the state. For the purposes of this study, the author has chosen the formation tops within the study area to agree with those in use by the North Dakota Geological Survey.

METHODS OF STUDY

For purposes of this study, data were collected primarily from mechanical well logs belonging to the North Dakota Geological Survey. To assure uniformity of correlation and data between wells, the spontaneous-potential log, the gamma-ray log, the resistivity log suite, and the dual-induction log were used most frequently.

All well logs, a total of 680, within the study area were used to construct a structure contour map of the top of the Rierdon Formation, an isopach map of the Swift Formation, and a map showing the location and thickness of the carbonate bodies studied. A total of 16 stratigraphic cross sections were prepared to show stratigraphic changes within the carbonate bodies.

Only one well within North Dakota, Terra Resources, Inc., Abrahamson #1-35 (NDGS Well No. 6179), has cored the lower half of the Swift Formation. The core from this well was studied in the North Dakota Geological Survey's Core and Sample Library. The core was examined and described using a hand lens, core slabs, and petrographic thin sections. X-ray diffraction and a scanning electron microscope were used to determine the mineralogy of the opaques within the core. Eighty-seven thin sections were studied with a reflecting binocular microscope. Select petrographic thin sections were stained with Alizarin Red Stain (Friedman, 1959) to differentiate calcite from dolomite. The carbonates were described using Dunham's (1962) classification, and the siliciclastics were described using Folk's (1974) classification.

Well cuttings are available from almost all wells drilled within the state, but, because of the inherent inaccuracies in the data resulting from using well cuttings, no detailed descriptions of the Swift Formation were made using cuttings. Samples from selected wells were examined to verify the presence or absence of carbonate fragments.

TYPE WELL-LOG CHARACTERISTICS

Mechanical well logs consisting of gamma-ray logs, spontaneous-potential logs, the resistivity log suite, and the dual-induction logs were used to determine thickness, structure, basic lithology, and correlation within the Swift Formation. Because of the local variability within the lower Swift Formation, four wells showing good log character and distributed across the study area were chosen as type logs (figs. 5, 6, 7, 8, and 9). NDGS Well Nos. 6834, 8089, and 8260 are located in areas of high well density. NDGS Well No. 6179 is located in an area of low well density.

The logs of all four type wells exhibited the same gross characteristics (figs. 6, 7, 8, and 9). Closer examination shows that the logs do have distinct differences, particularly within the lower three-fifths of the formation (units A-D). These differences will be discussed further in the following section concerning the Swift Formation.

Underlying Formation

The Rierdon Formation conformably underlies the Swift Formation throughout the study area. The contact between the Swift and the Rierdon is identified by a characteristic log marker called the "Rierdon Shoulder" (Francis, 1956, p. 31) (figs. 6, 7, 8, and 9), which is recognized by a sharp increase in the radioactivity of the gamma-ray log and a corresponding decrease in the resistivity readings upward. Below the "shoulder" and above the Piper Formation, the gamma-ray log and the resistivity log of the Rierdon Formation are convex toward

TABLE I

Review of Jurassic Nomenclature within the Williston Basin Area

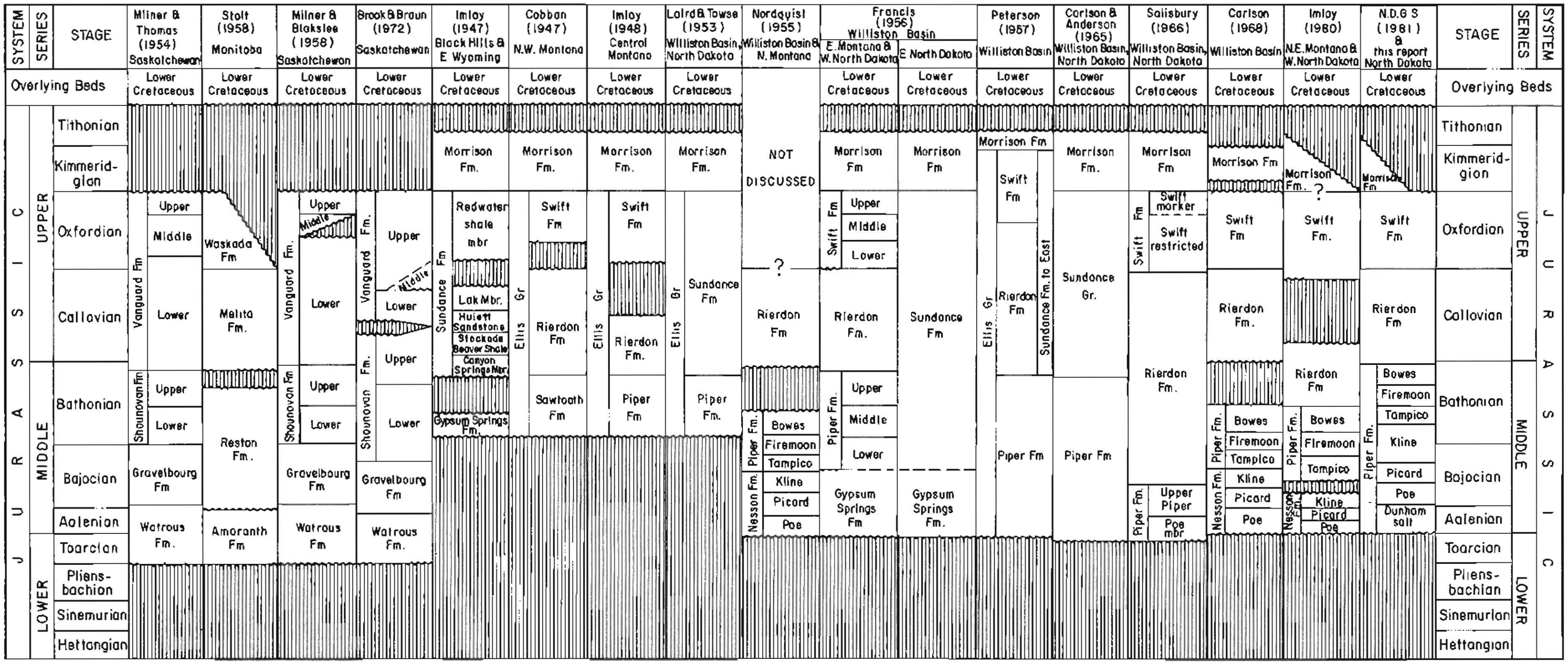

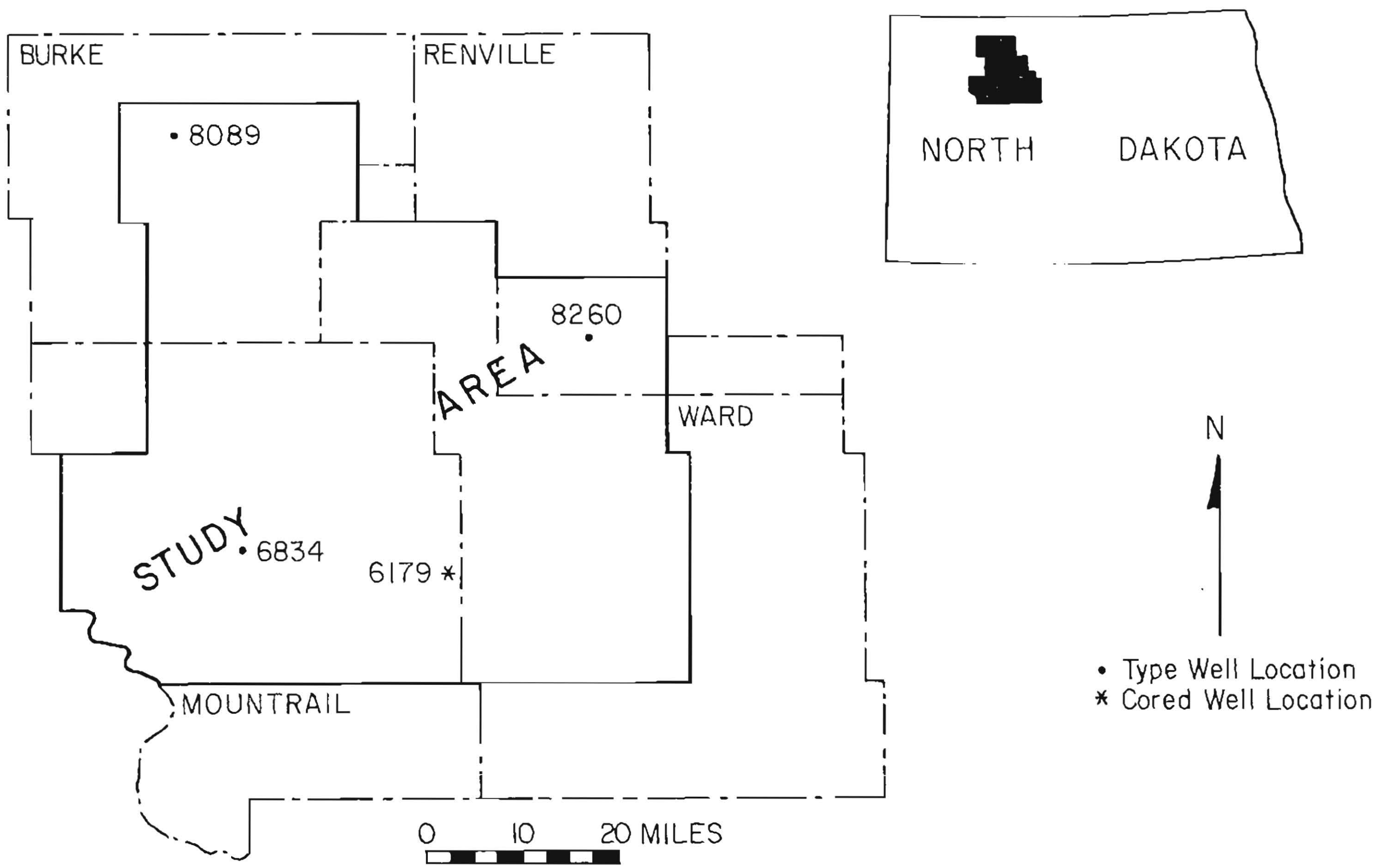

Figure 5. Location map of the type well logs used for correlation of the basal Swift Formation within the area of study.

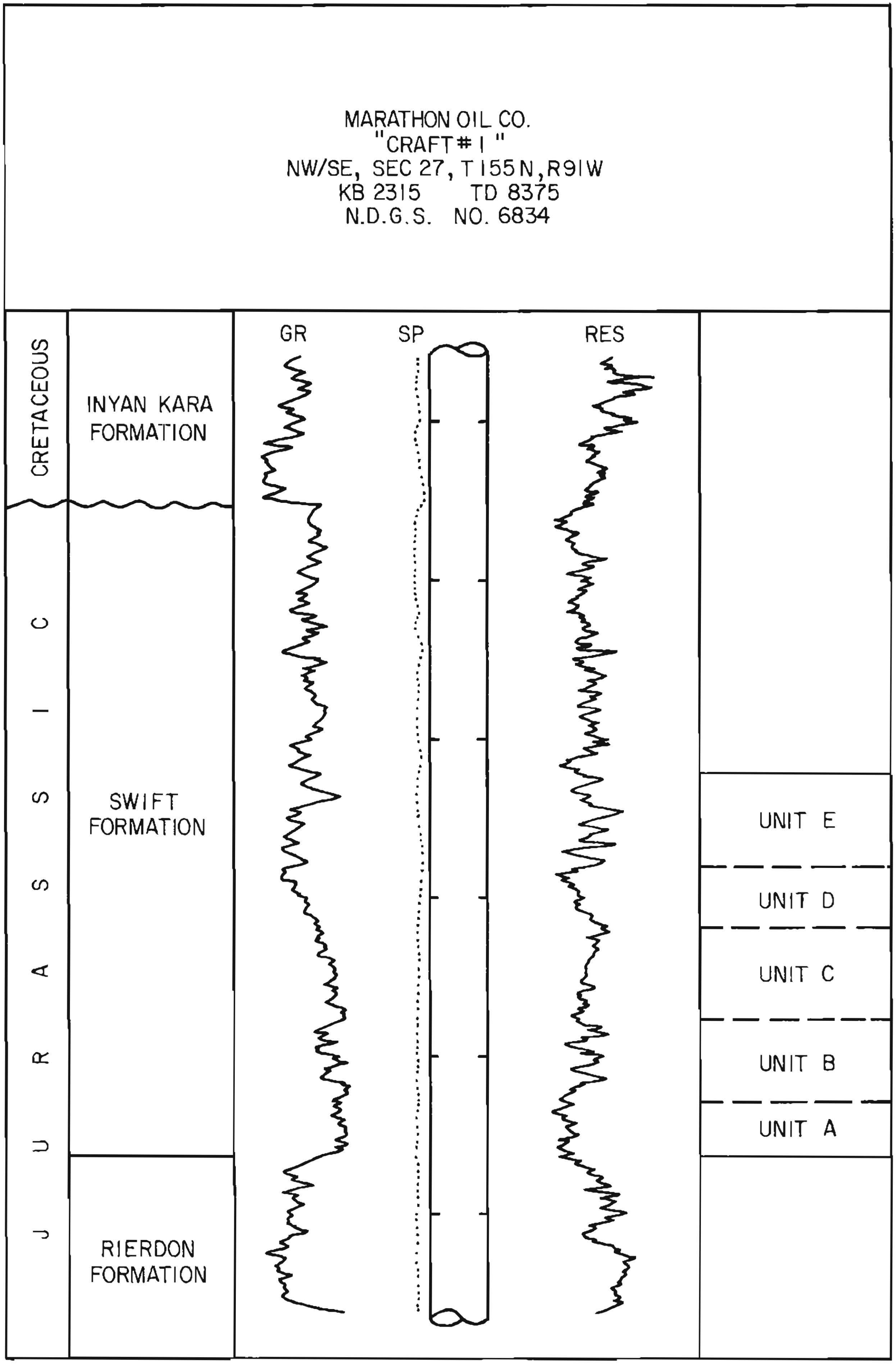

Figure 6. Typical gamma-ray log, spontaneous-potential log, and resistivity log of the Swift Formation, NDGS Well No. 6834, Mountrail County, North Dakota.

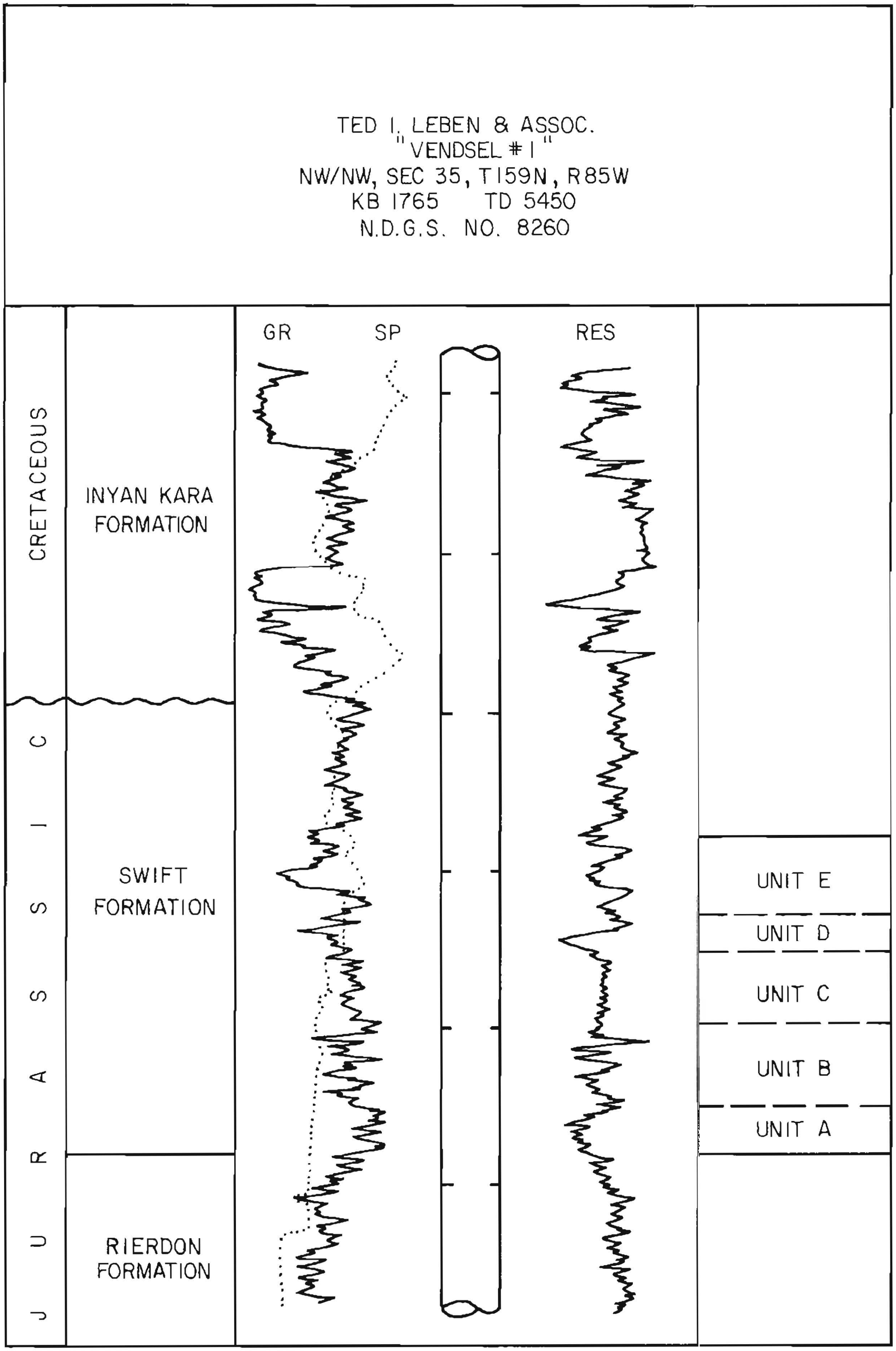

Figure 7. Typical gamma-ray log, spontaneous-potential log, and resistivity log of the Swift Formation, NDGS Well No. 8260, Renville County, North Dakota.

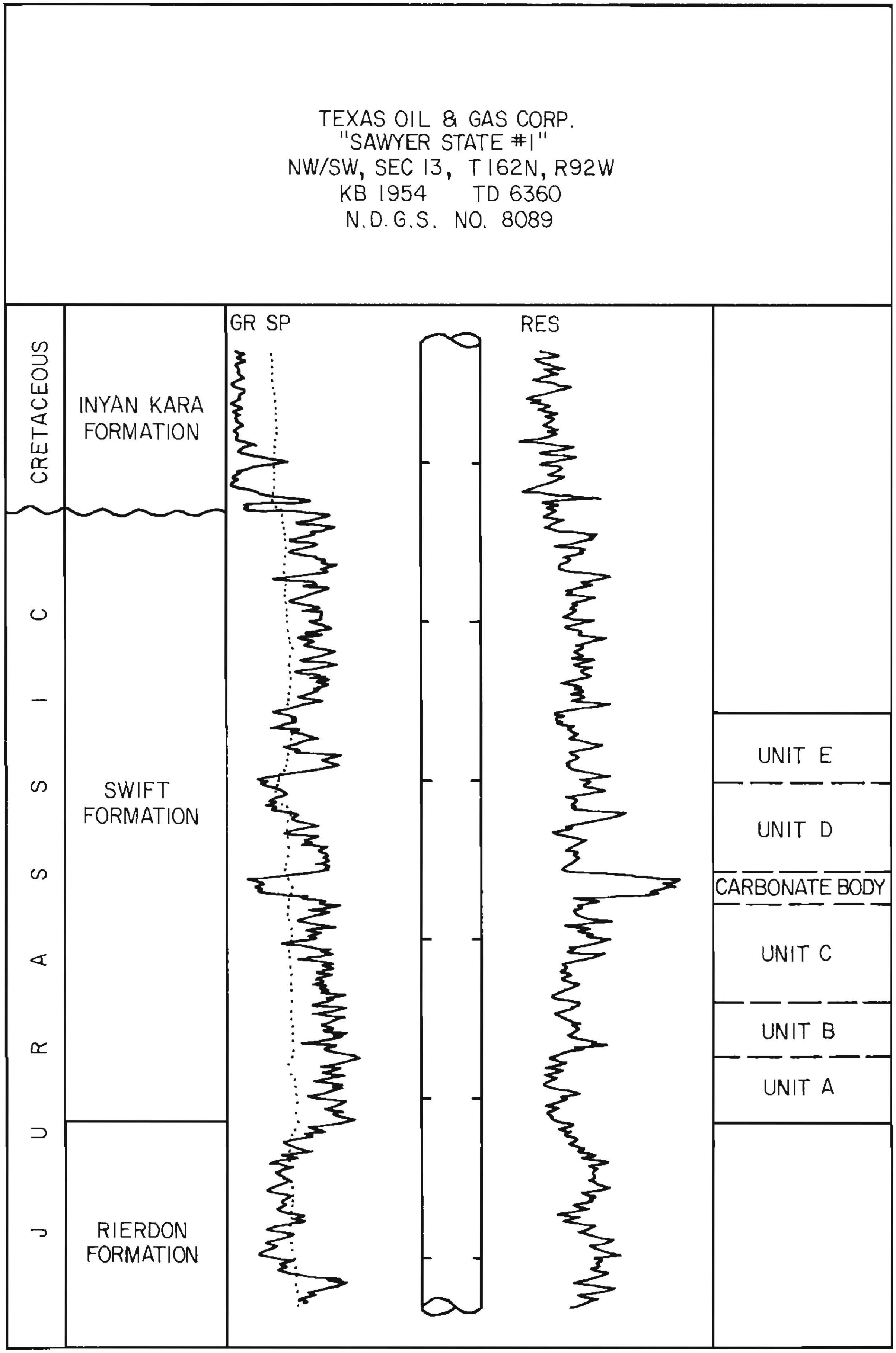

Figure 8. Typical gamma-ray log, spontaneous-potential log, and resistivity log of the Swift Formation, NDGS Well No. 8089, Burke County, North Dakota.

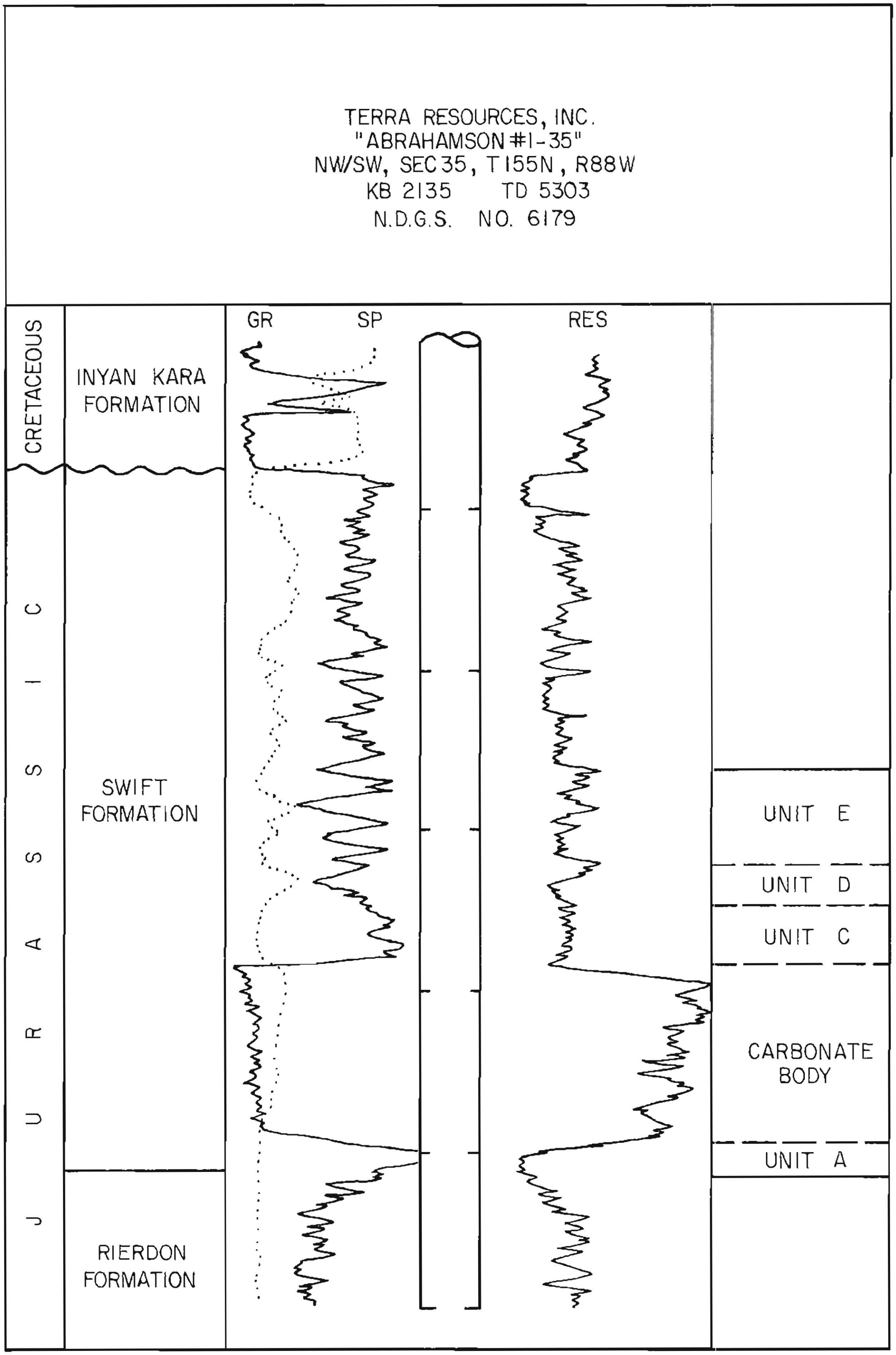

Figure 9. Typical gamma-ray log, spontaneous-potential log, and resistivity log of a carbonate body within the basal Swift Formation, NDGS Well No. 6179, Mountrail County, North Dakota.

the log boundaries.

Swift Formation

The overall log character of the Swift Formation is uniform throughout the study area. The basal portion of the Swift is recognized by its high gamma-ray readings and low resistivity readings. These characteristics gradually change upsection as the gamma-ray readings decrease and the resistivity increases slightly. No apparent, consistent change in the spontaneous-potential log occurs.

The major concern of this study has been the lower half to three-fifths of the Swift Formation. It is within this interval that the carbonate bodies and variability in log character occur. It should be noted that the units designated within the Swift (other than the carbonate bodies) were not chosen with detailed lithologic differentiation as the sole objective. In some cases, unit boundaries were based also on characteristic marker deflections, which were used for correlation purposes.

Characteristics of NDGS Well Nos. 6834 and 8260

Marathon Oil Company, Craft #1, NDGS Well No. 6834 and T. I. Leben and Associates, Vendsel et al. #1, NDGS Well No. 8260 show similar detailed log character in units A through D (figs. 7 and 8). Unit A is characterized by a highly radioactive gamma-ray log that is associated with low resistivity readings. Lithologically, these two criteria tend to be indicative of a mudstone or shale.

Three recognizable deflections make up unit B, and show a distinct change in log character from unit A. These deflections are characterized by a decrease in the gamma-ray log and an increase in the resistivity readings. This indicates an increase in coarser material in this unit.

Unit C corresponds to a gradational change in log character. The radioactivity tends to be higher at the base of unit C, and it decreases upsection as the corresponding resistivity increases. This indicates a return to a more shaly section than unit B and then a gradual increase in the concentration of coarser material near the top of unit C.

Unit D is characterized by a gradual decrease upward in the radioactivity of the gamma-ray log with an associated decrease in the resistivity log. These combined characteristics indicate a zone that is coarsening upward and contains decreasing quantities of shaly material upward. It is possibly developing some porosity.

Unit E is a zone that shows a low in the radioactivity of the gamma-ray log associated with a more active resistivity log. This unit reflects the predominance of silts and sands over finer clastics.

Characteristics of NDGS Well No. 8089

Texas Oil and Gas Corporation, Sawyer-State #1, NDGS Well No. 8089 (fig. 8) is located in the northwestern corner of the study area, the area of highest well concentration. Designations of units A through C are based primarily upon characteristic marker deflections on the resistivity log (fig. 8). Each of these deflections marks the beginning of a more resistive overlying unit: B is more resistive than A and C is more resistive than B. The gamma-ray logs in units A through C indicate a silty shale or mudstone.

Unit D is differentiated by an indicated decrease in radioactivity on the gamma-ray log. The character and lithology of this section closely correspond to unit C on NDGS Well Nos. 6834 (fig. 6) and 8260 (fig. 7). Unit D becomes clean (extremely low radioactivity) on the gamma-ray log and may assume a log character similar to that of the carbonate bodies. The resistivity curve has a sporadic character, and varies between high and low readings. This unit is not considered to be a carbonate, but a siliciclastic sand. Lithologic logs describe unit D as a quartzose sand with occasional thin limy stringers.

The last unit on Well No. 8089 (fig. 8) is recognized by a characteristic indicated increase in the radioactivity on the gamma-ray log. A sharp increase followed by a decrease in the radioactivity mark the boundary between units D and E. Although the radioactivity log shows a gradual decrease in unit E, this is not always the case, as a sudden increase in the resistivity may occur. Unit E tends to correspond closely to the upper portion of unit D on NDGS Well Nos. 6834 (fig. 8) and 8260 (fig. 7).

Between units C and D (fig. 8), a

sharp decrease in the radioactivity occurs with a corresponding increase in the resistivity. This reflects the log character of the carbonate bodies, as initially described by Moore and Anderson (North Dakota Geological Survey; personal commun., 1980), and recognized by the present author.

Characteristics of NDGS Well No. 6179

Terra Resources, Inc., Abrahamson #1-35, NDGS Well No. 6179 (fig. 9) is the only well within the study area with a core that has penetrated a Swift Formation carbonate body. Units A, C, and D correspond to the same units on Well Nos. 6834 (fig. 6) and 8260 (fig. 7). A carbonate body replaces unit B in this well.

The log for the Abrahamson well (fig. 9) shows a decrease in the radioactivity of the gamma-ray log with a corresponding increase in the resistivity log that is associated with the base of the carbonate bodies. Little change occurs in the gamma-ray curve upsection until the upper ten feet of the carbonate body are reached, at which point the radioactivity decreases again. The resistivity readings gradually increase upward with a sudden increase in the top ten feet. The spontaneous-potential log gradually reverses upward through the carbonate body, with a maximum reversal occurring in the upper ten feet. This reversal is indicative of formation fluids that are fresher than the drilling fluids.

The upper contact of the body with the overlying sediments is recognized by a sharp increase in the radioactivity, and a notable shift of the spontaneous-potential log back to a mudstone or a shale.

Overlying Formation

The Lower Cretaceous Inyan Kara Formation unconformably overlies the Swift Formation throughout the study area. The Swift-Inyan Kara contact is difficult to distinguish on some of the mechanical well logs. Generally the contact can be associated with one or more of the following: a decrease in the radioactivity of the gamma-ray log (figs. 6, 7, 8, and 9), a positive shift in the spontaneous-potential log (figs. 6 and 9), or a sharp increase or decrease in the resistivity log (figs. 8 and 9).

The Inyan Kara is recognized by an erratic self-potential log, actively changing resistivity readings, and alternating increases (shales or mudstones) and decreases (sands) in the radioactivity of the gamma-ray log.

RESULTS OF THE MECHANICAL WELL-LOG DATA

General Statement

Data gathered from the mechanical well logs were used to construct a series of subsurface maps and stratigraphic cross sections. A structure contour map of the top of the Rierdon Formation, an isopach map of the Swift Formation, and a map of the location and thickness of the carbonate bodies within the lower Swift were constructed.

A total of 16 stratigraphic cross sections were constructed within the study area (pl. 3). Of the 16 cross sections, six (three east-west and three north-south) were constructed to give an overall view of the general stratigraphy of the Swift Formation and its relationship to the surrounding formations. The remaining 10 cross sections were constructed through the major fields within the study area (table 2). These cross sections provide the necessary detail to critically evaluate the stratigraphic positions of the bodies and their relationship to the surrounding units.

Areal Extent and Thickness of the Swift Formation and Its Carbonate Bodies

The Swift Formation is found only in the subsurface in North Dakota and is thickest near the center of the western half of the state.

The thickness of the Swift Formation in the study area ranges from 264 feet in the northeastern corner to 497 feet in the southwestern corner (pl. 1). Isolated areas of thickening and thinning occur throughout the study area. These areas are most likely related to the post-Swift--pre-Inyan Kara erosional surface, and possibly to differential Dunham Salt dissolution (Salisbury, 1966).

The preliminary subsurface study identified 53 carbonate bodies of similar log character, widely scattered across the western half of North Dakota (fig.

TABLE 2.--Location of Stratigraphic Cross Sections within the Area of Study.

Area	Cross Section	Plate Number
Regional	A-A', B-B'	5
	C-C', D-D'	6
	E-E', F-F'	7
Stanley Field	G-G'	8
	H-H'	9
Berthold Field	I-I'	10
Lonetree Field	J-J', K-K'	11
South Lonetree Field		
Donnybrook Field	L-L'	12
Southwest Aurelia Field		
Chola Field	M-M'	13
Lake Darling Field	N-N'	14
Macobee Coulee Field		
Lockwood Field		
Black Slough Field	O-O'	15
Foothills Field	P-P'	16
Northeast Foothills Field		
Lignite Field		
Rennie Lake Field		
Rival Field		
Woburn Field		

3). Twenty-one of these 53 bodies, which were found within close proximity of one another, occur within the study area.

The detailed examination of all of the available well logs within the study area resulted in the recognition of a much larger number of these bodies characterized by very low radioactivity readings and associated very high resistivity readings. Plate 2 shows the areal extent and thickness of these bodies. They tend to be widely scattered throughout the study area, and they are much more extensive than the initial investigation of the state suggested. In those wells penetrating a carbonate body, only one body was present. No multiple bodies of carbonate were encountered. Due to the regional changes in the stratigraphic position and the local variability in their thickness, no continuous upper or lower boundaries could be determined. It should be noted that the location and thickness map of the carbonate bodies (pl. 2) is not an isopach or an isochore map, but simply a map showing the thickness of total carbonate within the basal Swift Formation.

The variability in the thicknesses of carbonate bodies within the lower Swift Formation is noteworthy (pl. 2). Only six well logs show a body over 100 feet thick (table 3). Of these six bodies, the maximum thickness penetrated was 155 feet (NDGS Well No. 6289). Most bodies recognized were less than 50 feet thick, and the thinnest was four (NDGS Well Nos. 4406 and 8204).

Regionally, the carbonate bodies have a predominantly north-northeast to south-southwest trend or a north-northwest to south-southeast trend with a limited east-west extent (pl. 2). Within some of these elongate trends, distinct pods or mounds of thicker carbonate, separated by the thinning or complete absence of carbonate, can be delineated. These areas of thicker

TABLE 3.--Wells with Swift Carbonate Bodies over One Hundred Feet Thick.

NDGS Well No.	Operator and Name	Location	Thickness
6289	Brooks Exploration, Inc. Harstad et al. #1	NESW-10-155-91	155 ft.
6734	Brooks Exploration, Inc. Harstad #10-1	NWSE-10-155-91	135 ft.
6376	Brooks Exploration, Inc. Harstad et al. #2	SWSE-10-155-91	108 ft.
2816	Davis Oil Co. Len Carkuff #1	SWSE-12-154-92	110 ft.
6295	Hawn Brothers Arne Haaland #1	NENE-35-157-87	106 ft.
*6179	Terra Resources, Inc. Abrahamson #1-35	NWSW-35-155-88	109 ft.

* Core

carbonate are somewhat elliptical in nature, with their longer axis trending slightly perpendicular to the overall trend. This is particularly true in the eastern part of the study area.

Comparing the isopach map of the Swift Formation (pl. 1) with the map of total carbonate thickness (pl. 2) reveals some possible relationships between the two. In making these comparisons, it should be kept in mind that the effects of differential salt solution and the post-Swift erosional surface on the present configuration of the Swift isopach map cannot be fully assessed.

The most striking correlation occurs along the 400-foot isopach of the Swift Formation and the zero limit of the carbonates to the west and south of Donnybrook, Berthold, Lonetree, and South Lonetree Fields in the eastern part of the study area. In this area the carbonate bodies occur where the Swift Formation is slightly thinner (< 400 feet) and they are absent in areas where the Swift becomes noticeably thicker (> 400 feet). The relationship between the location and thickness of the carbonate bodies and the changing thickness of the Swift Formation might indicate that a shelf edge or break in the basin topography was present here during the deposition of the lower Swift.

In other localized areas, the opposite seems to be true; the carbonate bodies seem to occur where the Swift Formation is showing some thickening. The area in and around the Stanley Field best demonstrates this situation. Three of the thickest carbonate bodies penetrated in the study area coincide with a noticeable thickening of the Swift Formation in this local area. This might imply that the thickening of the Swift Formation in the Stanley Field, and in other similar areas, was due to the presence of the thick carbonate bodies or lows within the top of the Rierdon Formation.

Characteristics of the Carbonate Bodies

Log Character

The mechanical well-log character of the carbonate bodies located within the study area is, in most cases, similar to the well log of the Abrahamson #1-35 (fig. 9). Recognition of the gradual coarsening-upward character of the unit is limited in the thinner (0-20 feet) carbonate bodies. These thinner bodies are distinguished on logs by the very low gamma-ray log readings and associated high resistivity readings.

Although the overall well-log character of the bodies remains fairly consistent within the study area, locally there are changes in the well-log character of the carbonate bodies within the Berthold, Lonetree, and South Lonetree Fields (pls. 3, 10, and 11) because of changes in the carbonate bodies there. The well logs in this area show the same overall low radioactivity readings and coarsening-upward log character previously described. The upper and lower contacts of the carbonate bodies are still distinguished by the same changes in the gamma-ray log and the resistivity log described in the type Well No. 6179 (fig. 9).

Relationship of the Carbonate Bodies to the Underlying Formation

No relationship between the structure on top of the Rierdon Formation and the presence of the carbonate bodies was established. No consistent correlations between the occurrence of the carbonate bodies and the paleostructure on top of the Rierdon Formation were made. The first reliable and locally continuous log markers available are indicated approximately 250 feet above the top of the "Rierdon Shoulder." Some minor structural changes in the Rierdon surface are indicated on cross sections hung on these local markers. It is possible that structural changes could have occurred after deposition of the Rierdon but prior to the accumulation of the sediments represented by the marker.

Stratigraphic Position of the Carbonate Bodies

Throughout the study area the carbonate bodies are limited to the basal 150 feet of the Swift Formation. Toward the northern and northeastern portion of the study area, the bodies seem to occur higher within the lower Swift section (pl. 6, C-C'; pl. 14, N-N'; pl. 15, O-O'; and pl. 16, P-P').

Those carbonate bodies found within the Berthold, Lonetree, and South Lonetree Fields (pl. 10, I-I'; and pl. 11, J-J', K-K'); the Donnybrook to Southwest Aurelia Fields (pl. 12, L-L'); and the northernmost corner of the study area (pl. 15, O-O'; and pl. 16, P-P') illustrate that variation in stratigraphic position may occur by area. For example, the carbonates present within the Berthold, Lonetree, and South Lonetree Fields (pl. 10, I-I'; and pl. 11, J-J', K-K') occur 0 to 20 feet above the Rierdon Formation, whereas in the fields in the northwestern corner of the area (pl. 15, O-O'; and pl. 16, P-P') the carbonate bodies occur 130 to 150 feet above the top of the Rierdon Formation. The bodies occur approximately 30 to 70 feet above the base of the Swift Formation between these two areas. Note that because of the greater lateral extent of cross section L-L' (pl. 12), more than one carbonate body is encompassed.

Units A, B, and C of the Swift Formation are most affected by the occurrence of the carbonate bodies. The carbonate bodies most often replace units B and C, but some of the thicker carbonates do involve unit A. The carbonate bodies occur at the expense of these three units so that little noticeable increase in the overall thickness of the Swift Formation is observed.

The upper contact of adjacent carbonate units rarely occurs in the same stratigraphic position. Within the study area, the upper contact of the bodies occurs anywhere within the basal 150 feet of the Swift Formation, but in no place does it extend into unit D. Some of the thicker carbonate bodies and those bodies occurring higher in the section seem to terminate within 30 feet of unit D (pl. 6, C-C'; pl. 9, H-H'; pl. 10, I-I'; pl. 12, L-L'; pl. 13, M-M'; pl. 14, N-N'; pl. 15, O-O'; and pl. 16, P-P').

Relationship Between the Carbonate Bodies and the Surrounding Formations and Units

Rierdon and Inyan Kara Formations

As already noted, no absolute statement can be made concerning the relationship between the carbonate bodies and the Rierdon paleostructure. The configuration of the Swift-Inyan Kara contact is not affected by the presence of individual carbonate bodies. Throughout most of the study area this contact shows some relief. Along the eastern margin of the study area, the contact between the Swift and the Inyan Kara becomes noticeably more irregular (pl. 5, A-A', B-B'; pl. 7, F-F'; pl. 13, M-M'; and pl. 14,

TABLE 4.--Summary of Textures, Sedimentary Structures, and Diagenesis Recognized within the Abrahamson #1-35 Core.

FACIES	Packstone-Grainstone Facies	Shale-Mudstone-Siltstone-Quartzarenite Facies
ALLOCHEMS/ GRAINS	Pelecypods, gastropods, echinoderms, superficial oolites, oolites, intraclast peloids, unidentifiable allochems, siliciclastic sand	Quartz, feldspar, glauconite opaques, mollusks, echinoderms, intraclasts
GRAIN SIZE	Very fine grained to coarse-grained: coarsens upward	Shales to medium-grained: coarsens upward
SHAPE	Well-rounded bioclasts, subangular to subrounded sands	Subangular to subrounded grains
SORTING	Overall, moderately poor sorting; individual laminations are well sorted	Moderately poor sorting to well-sorted
POROSITY	Moldic: completely infilled, partially infilled, open; intercrystalline	Interparticle
CEMENT/ MATRIX	Micrite, microspar, pseudospar, isopachous calcite	Clays, calcite
SEDIMENTARY STRUCTURES	Trough cross-laminations, parallel cross-laminations, imbrication, reactivation surfaces, massive, low-angle laminations, bioturbation?	Massive, fissile, ripples, trough cross-laminations, planar parallel laminations, bioturbation
DIAGENESIS	Aggrading neomorphism, alteration siliciclastics, stylolitization, compaction, recrystallization, dissolution, silicification, dolomitization	Compaction

The matrix from 5,195 to 5,094 feet consists of micrite mud that has partially aggraded to microspar and pseudospar. The micrite mud is most common at the base of the facies, while the amounts of microspar and pseudospar increase upward.

The interval from 5,094 to 5,091 feet contains both micrite mud and primary isopachous calcite cement between the grains. This has been designated a mixed packstone-grainstone zone, and it is the gradational unit between the packstone interval and the grainstone interval.

The top 5 feet between 5,091 and 5,086 feet of the packstone-grainstone facies is a grainstone. These grains are isopachously cemented by calcite. Small equant calcite anhedra generally fill the remaining space between the grains, but in some places minor intercrystalline porosity is observed. Silica and anhydrite (gypsum ?) have completely filled the molds within a localized area at the very top of the facies. Some pores within the packstone-grainstone facies have been infilled with sparry calcite and insoluble debris that has been dissolved

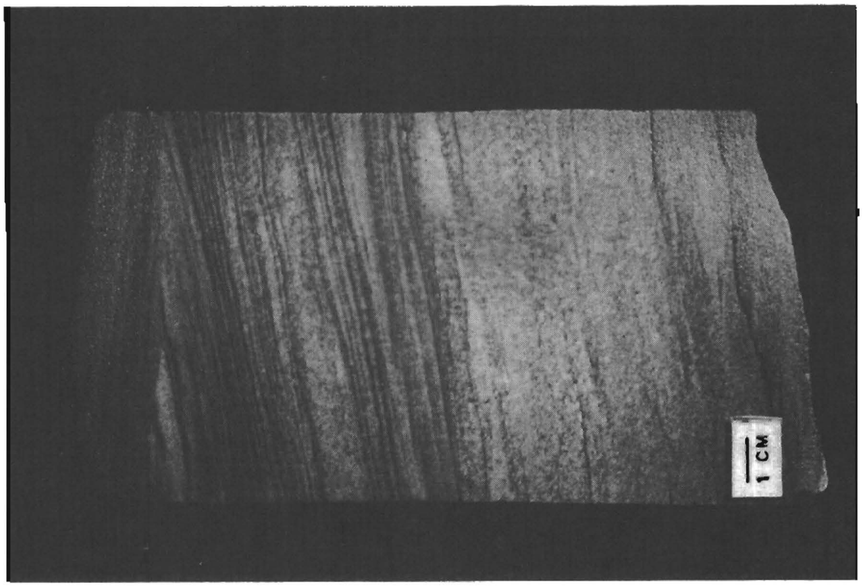

Figure 13. Core slab of the cross-laminated glauconitic quartzarenite which conformably underlies the packstone-grainstone facies. 5195.1 to 5194.5 feet.

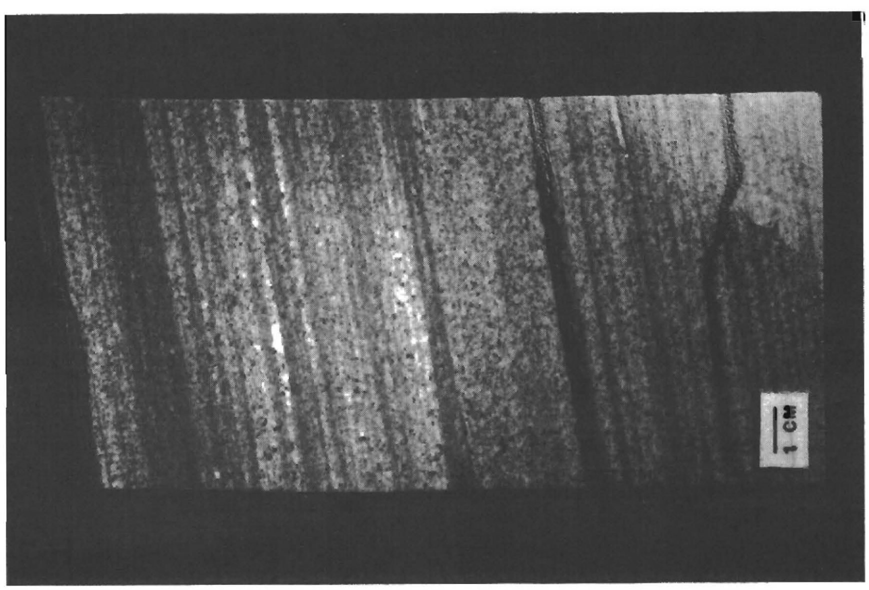

Figure 14. Core slab showing the gradational change from the glauconitic quartzarenite to the packstone-grainstone facies. 5192.0 to 5191.5 feet.

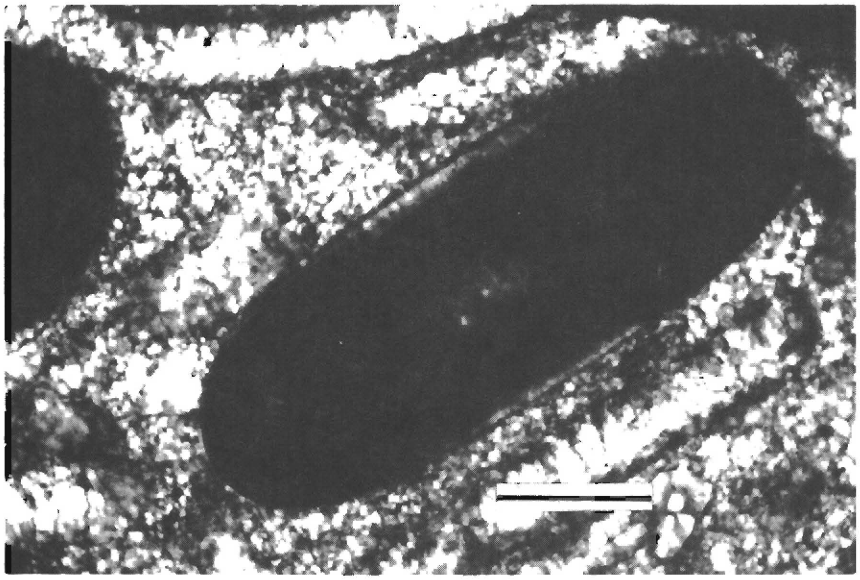

Figure 15. Photomicrograph of an unidentifiable fossil (?) allochem. Thin-section number 5127.2, 100X. Bar represents .2 mm.

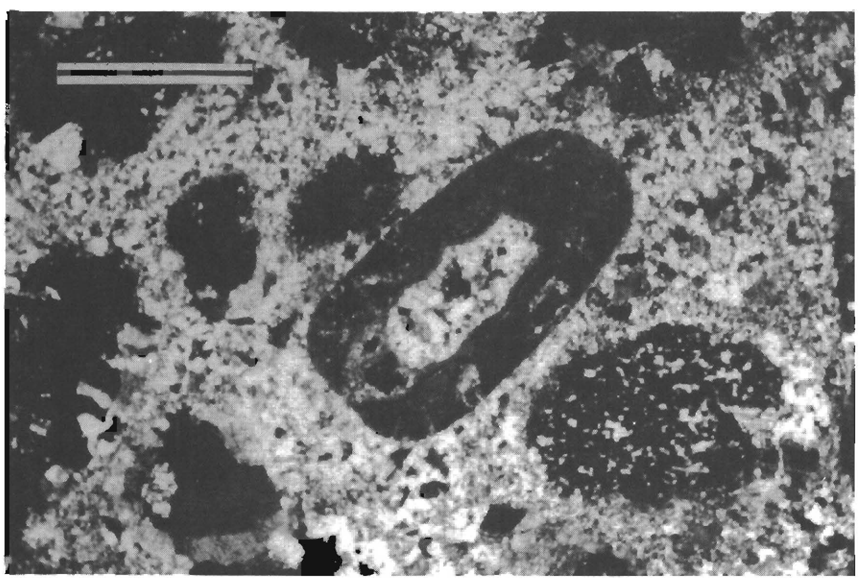

Figure 16. Photomicrograph of an unidentifiable fossil (?) allochem. Thin-section number 5109.8, 40X. Bar represents .5 mm.

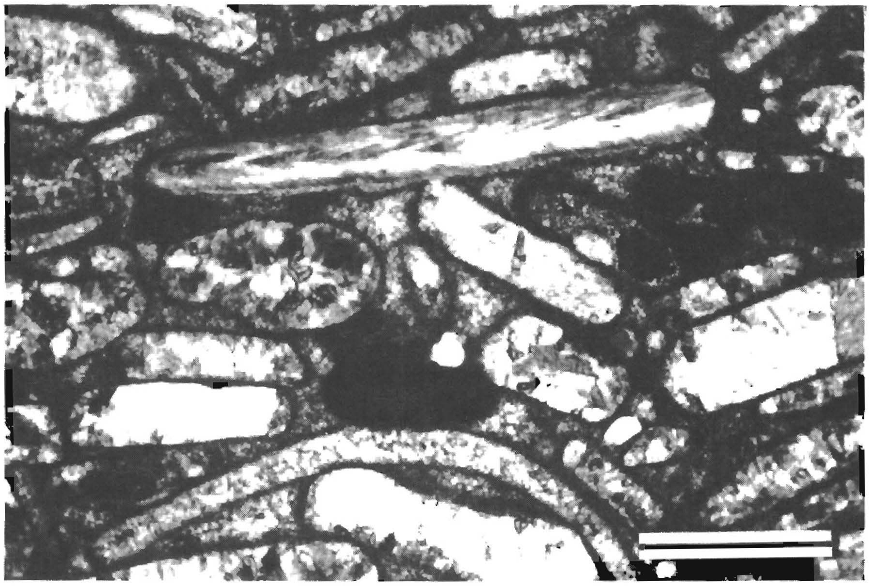

Figure 17. Photomicrograph of a thin section taken parallel to the length of the core showing the elongate shape of the allochems. Thin-section number 5135.1, 40X. Bar represents .5 mm.

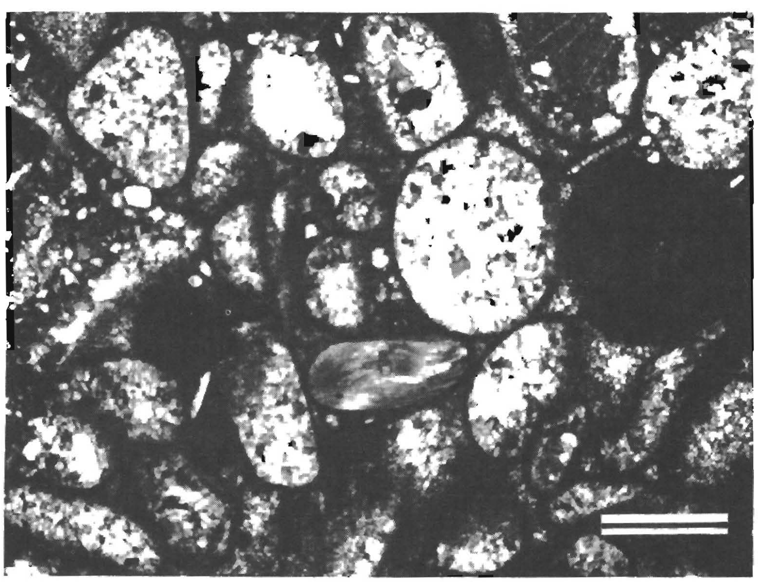

Figure 18. Photomicrograph of a thin section taken normal to the length of the core showing the discoid shape of the allochems. Thin-section number 5135.4, 25X. Bar represents .5 mm.

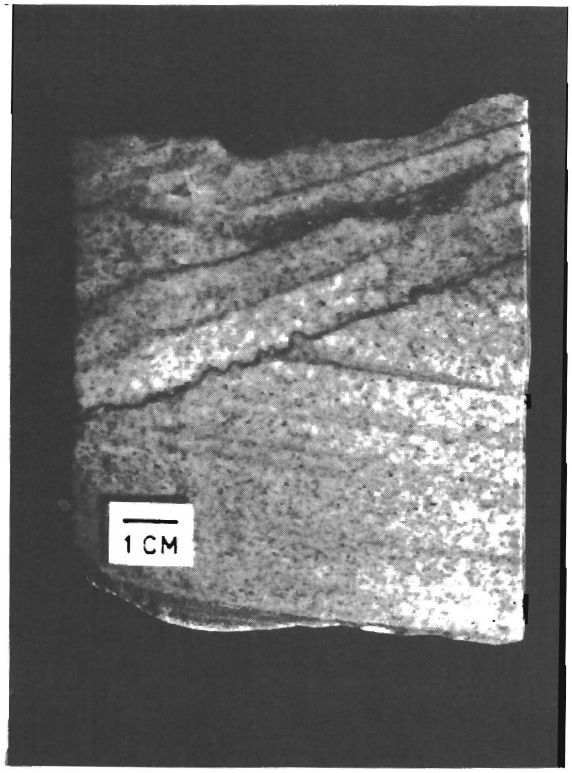

Figure 19. Core slab showing a reactivation surface with laminations dipping 22°. Core slab 5120.8 to 5120.6 feet.

from the surrounding rock.

Sedimentary Structures

Laminations are the most common sedimentary structure within the packstone-grainstone facies. The laminations are usually parallel cross-laminations that have a range of dips from 2° to 10°. The maximum inclination of the parallel laminations was found to be 22° (Harms and others, 1975) (fig. 19) on laminations directly overlying a reactivation surface.

These laminations may be ripple cross-laminations which occur in areas of wave and/or current activity and sediment transport (Campbell, 1971; Clifton, Hunter, and Phillips, 1971). They could also be what Harms and others (1975, p. 87) call "hummocky cross-stratification." This is recognized by poorly organized, low-angle cross-laminations ($< 15°$) composed of very fine to fine sands. The sets of cross-laminae have lower boundaries that are erosional with the underlying laminae and are parallel to the erosional surface. Dip directions of the laminae are random. Hummocky cross-stratification is common in the deposits of the lower shoreface and offshore, and is presumably formed during storm conditions (Harms and others, 1975; Hunter and Clifton, 1982).

Poorly formed trough cross-laminations were recognized near the top of the facies. No large-scale cross-stratification was recognized.

The laminations consist of alternating concentrations of very fine green sands and bioclastic grains. Very thin gradational boundaries separating adjacent laminations can be recognized.

Overall, the packstone-grainstone facies is inversely graded. This is particularly true of the mollusk fragments. Inverse grading rarely occurs within individual laminations although, when present, the grading generally involves a change between two grain sizes on the Wentworth scale.

Reactivation surfaces indicating an interruption in the flow direction or deposition of the sands are also present (fig. 19). Most of these are very obscure and recognition is based primarily upon distinct changes in the direction of dip on the laminations.

Imbricate mollusk grains are prominent throughout the facies. Imbrication is primarily a function of the elongate, discoid shape of the grains

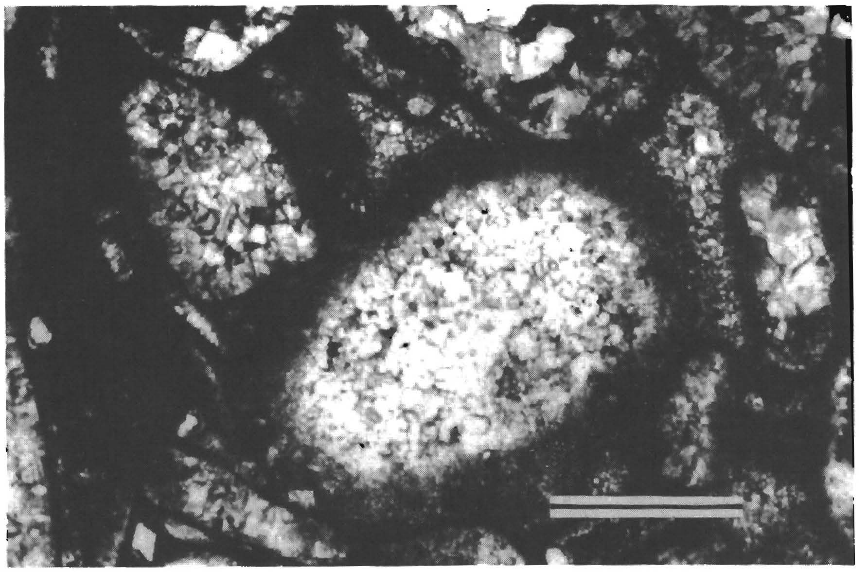

Figure 20. Photomicrograph of a burrow (?) within the packstone-grainstone facies. Thin-section number 5148.8, 40X. Bar represents .5 mm.

and their response to the direction of current flow.

Little evidence of bioturbation exists within this facies. Uncommonly, circular to semi-elliptical clusters of equant sparry calcite with thick micrite rims are recognized (fig. 20, p. 70). These may be remnants of burrows, but the small size argues against this possibility.

Diagenesis

Diagenesis has been defined as "all changes experienced by sediments subsequent to deposition and prior to metamorphism" (Purdy, 1968, p. 184). Several post-depositional changes are evident within the packstone-grainstone facies.

The most prominent diagenetic fabrics are the moldic porosity, the mold infillings, and the aggrading neomorphism (Folk, 1965). Almost 95 percent of the mollusk grains appear to have undergone complete or partial dissolution developing an early moldic porosity (fig. 21). The original size and shape of the grains has been preserved by the presence of a micrite rim around each grain (Friedman, 1975).

The early molds within the packstone portion of this facies have been completely infilled and no pore space remains. Generally, only one episode of cementation of the molds can be seen in thin section. The infilling cement may be recognized as a very faint drusy calcite cement around the outer edge of the mold, which grades to a coarse sub-equant calcite cement filling the remaining pore space. Occasionally, a distinct and well-developed drusy calcite cement may be observed rimming the edge of these molds. One or two anhedral crystals of blocky calcite may fill the remaining pore space (fig. 22).

The molds within the grainstone portion of the facies (5,091 to 5,086 feet) show no infilling cement, a complete infilling cement, or, most commonly, a dog-tooth spar rim cement (figs. 23 and 24).

Aggrading neomorphism (Folk, 1965) within this facies is shown as micrite mud (original mineralogy unknown) aggraded to microspar and to pseudospar within the upper portion of this facies (fig. 22).

Features related to dissolution and compaction occur throughout the packstone-grainstone facies. Stylolites are extensive and are commonly found to be related to the formation of cavities filled with sparry calcite and insoluble debris. The dissolution of the carbonate material is related to the breakup of some of the very fine sands found

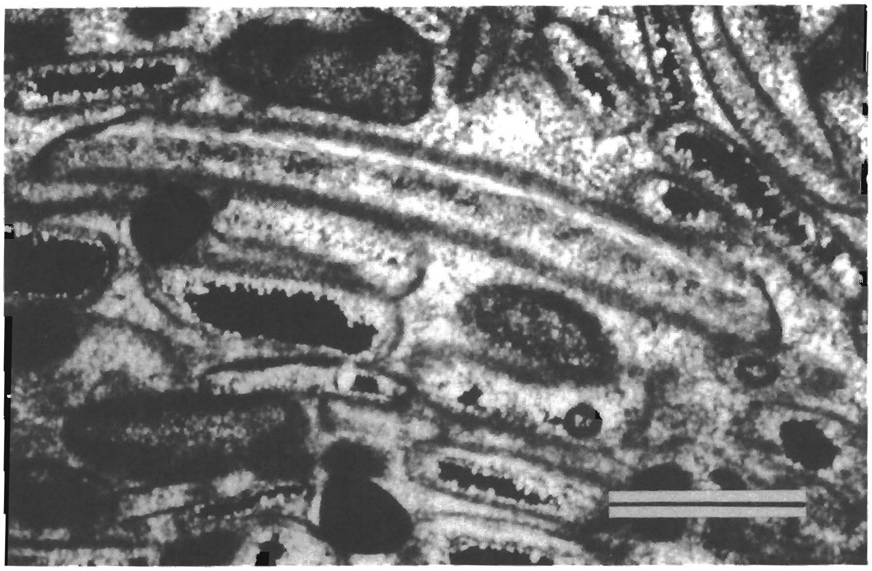

Figure 21. Photomicrograph of a partially recrystallized mollusk grain and the surrounding moldic porosity. Thin-section number 5093.9, 40X. Bar represents .5 mm.

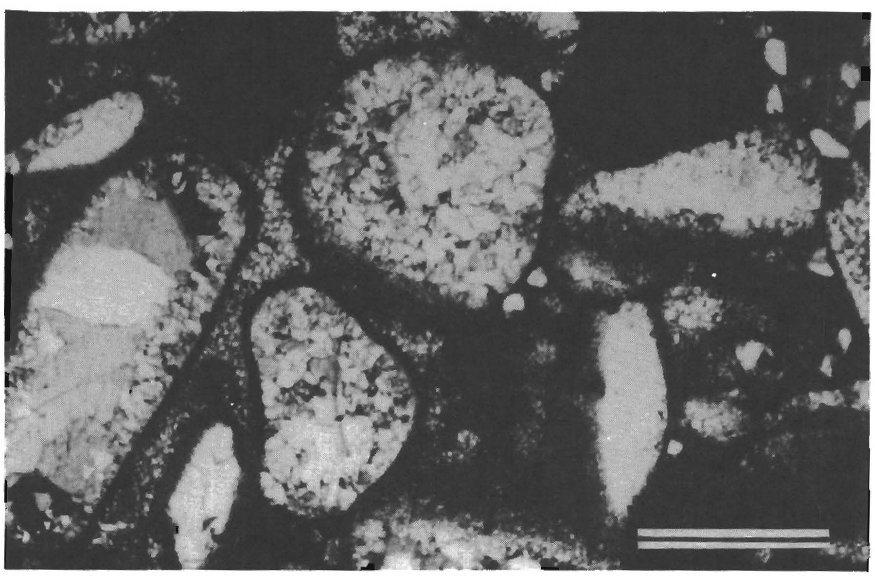

Figure 22. Photomicrograph of calcite cement infilling molds of mollusk grains. Thin-section number 5181.1, 40X. Bar represents .5 mm.

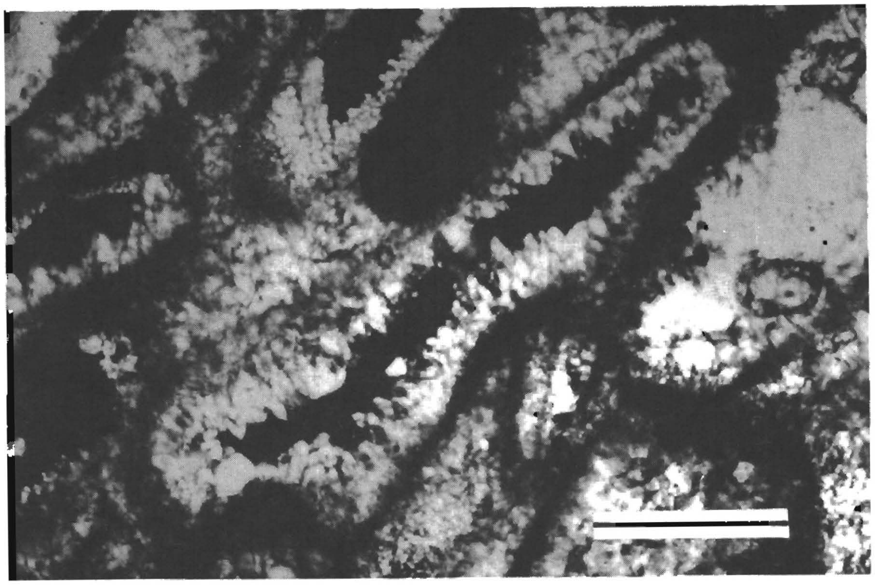

Figure 23. Photomicrograph of the dog-tooth spar infilling a mold of a mollusk grain within the grainstone portion of the packstone-grainstone facies. Thin-section number 5093.9, 100X. Bar represents .2 mm.

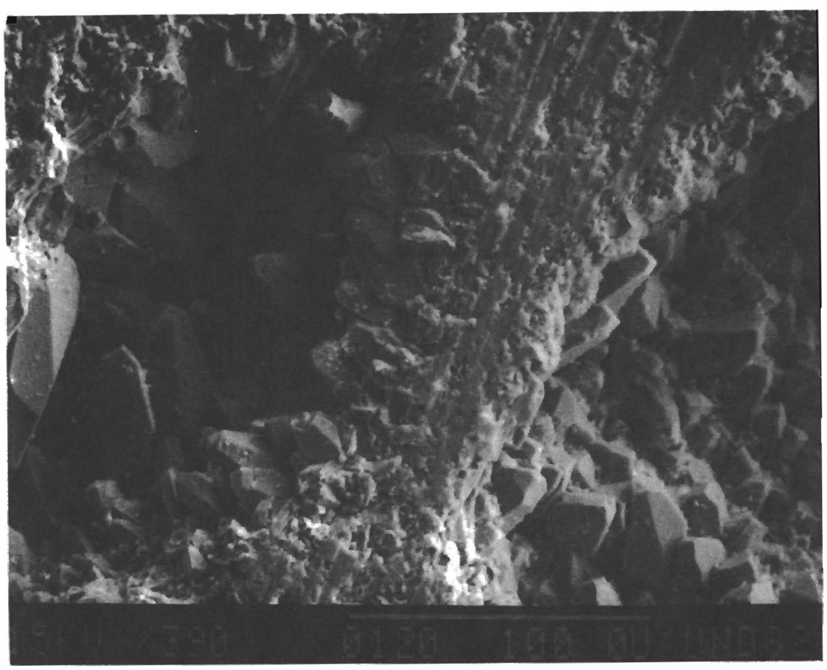

Figure 24. Scanning electron microscope photo of a mold partially infilled with dog-tooth spar.

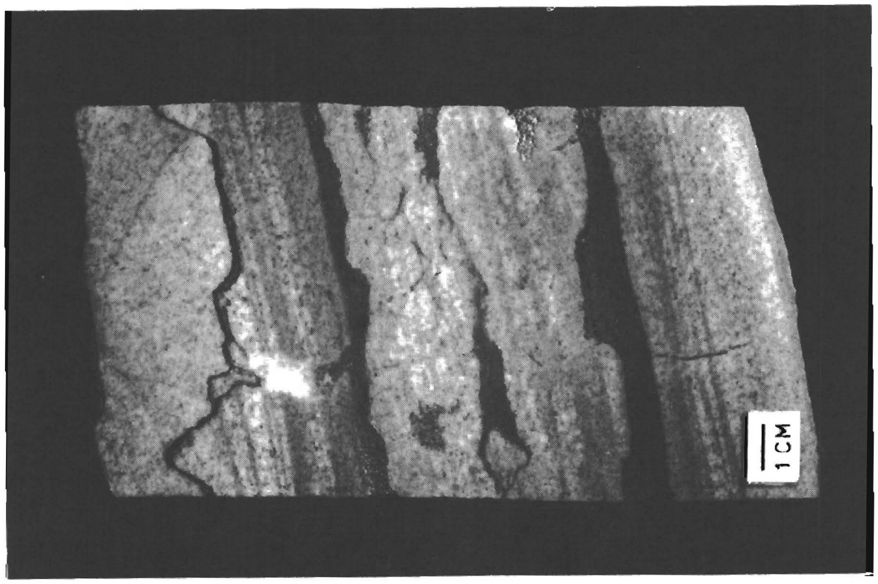

Figure 25. Core slab showing irregular laminations related to the dissolution and compaction of the surrounding packstone. 5157.3 to 5156.7 feet.

within the matrix into irregular laminations (fig. 25). Other minor features, such as fracturing and faulting, are recognized and are related to dissolution and compaction.

Partial replacement of a few carbonate grains by silica has occurred. Silicification has been both a primary (replacing grains with the original internal structure still present) and a secondary (replacing the calcite infilling of the molds) diagenetic change.

Staining with Alizarin Red Stain (Friedman, 1959) shows that dolomite is absent within the lower 100 feet of the packstone-grainstone facies, but is present within the upper 9 feet of the facies. The dolomite is restricted to the cement lining those grains still exhibiting remnant moldic porosity (fig. 26, p. 78).

Siliciclastic material partially altered to clays can be infrequently recognized.

Shale-Mudstone-Siltstone-Quartzarenite Facies

The shale - mudstone - siltstone - quartzarenite facies constitutes the upper 66 feet (5,086 to 5,020 feet) of the cored interval, and it unconformably overlies the packstone-grainstone facies (fig. 27). This facies coarsens upward from a shale to mudstone at the base, to a siltstone, and finally to a fossiliferous quartzarenite at the top.

Textures

The shale - mudstone - siltstone - quartzarenite facies is composed of mud, silt, medium sand, intraclasts, mollusk grains, and echinoderm fragments. Silt and medium sand are the most abundant constituents of this facies. These are predominantly monomineralic grains of quartz, feldspar, glauconite, and opaques. The silt and sand grains are generally subangular to subrounded, and are poor- to moderately well sorted.

Recognizable bioclastic material is limited to the coarser quartzarenite. The abraded material is angular, randomly scattered throughout the sand, and ranges in size from fine sand to very coarse sand.

The shales and mudstones contain

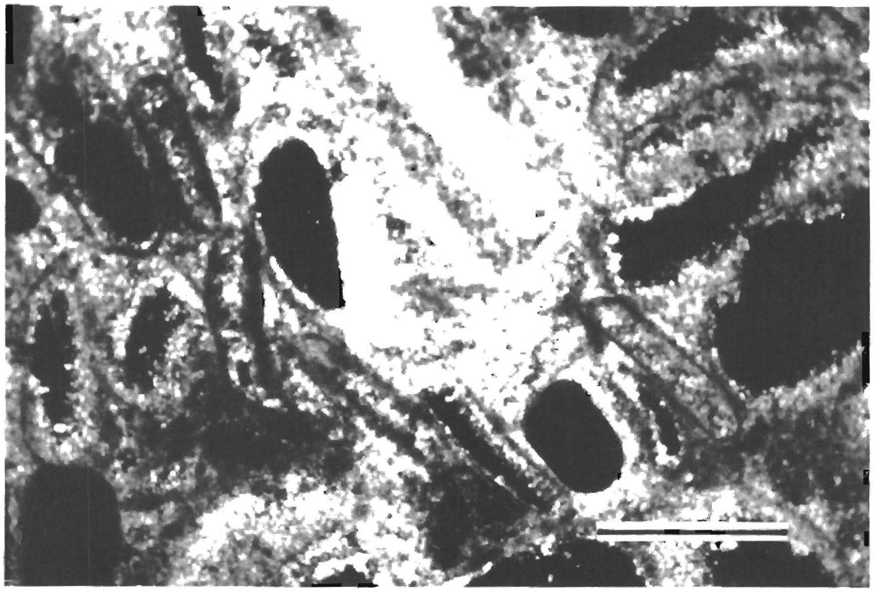

Figure 26. Photomicrograph of dolomite rim cement (D) partially infilling a mold within the grainstone portion of the packstone-grainstone facies. Thin-section number 5091.4, 40X. Bar represents .5 mm.

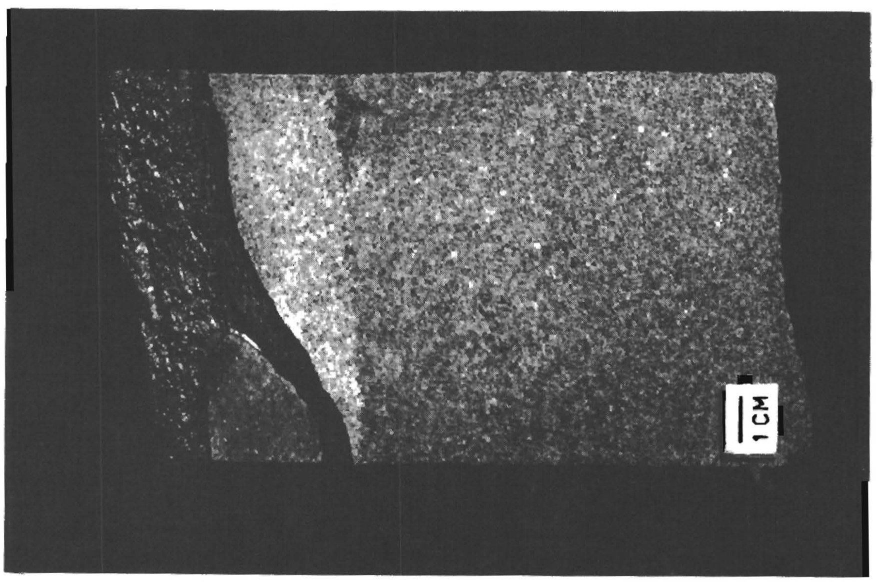

Figure 27. Core slab of the unconformity between the packstone-grainstone facies and the overlying shale-mudstone-siltstone-quartzarenite facies. 5086.3 to 5085.9 feet.

Figure 28. Core slab of a laminated and bioturbated quartzarenite. 5031.3 to 5030.5 feet.

varying amounts of silt and thin partings of green clay which swell on contact with water. These shales tend to be fissile and only slightly calcareous.

Intraclasts are present at the base of the shale-mudstone-siltstone-quartzarenite facies (fig. 27). The intraclasts are composed of bioclastic debris that is similar to the underlying packstone-grainstone facies.

The siltstone and quartzarenite portion of this facies shows primary interparticle porosity (Choquette and Pray, 1970). Some of the pores have been plugged by calcite cement and clays.

Sedimentary Structures

Trough cross-laminations and planar, parallel laminations are prominent throughout the shale-mudstone-siltstone-quartzarenite facies. Individual laminations may be separated by thin concentrations of clay and black organic (?) material, or may occur as alternating siltstones, quartzarenites, and mudstones (fig. 28, p. 81).

Small-scale ripples are present within the siltstone and lower quartzarenite portion of the facies. These ripples tend to be slightly asymmetrical to symmetrical, indicating oscillatory wave conditions, in addition to current activity. Climbing ripples are also present.

The upper portion of this facies shows evidence of having been bioturbated. Many of the laminations have been disturbed and cross-cut by vertical and horizontal burrows (figs. 28 and 29). Some burrows have been filled with waxy green clays, while others have been backfilled with the surrounding sediments. Concentrations of organics (?) and dark-brown clays tend to rim the burrows.

Diagenesis

Other than the bioturbation and cementation of the sediments, compaction and the formation of stylolites are the only apparent post-depositional changes that have occurred in the shale-mudstone-siltstone-quartzarenite facies. Thin stylolites are found along the edges of the larger mollusk and echinoderm fragments (fig. 30, p. 84), quartz sands can be seen penetrating the edges of the mollusk and echinoderm fragments, and bent and broken fossil debris is present.

DISCUSSION

Relationship of the Core to the Well Log

The mechanical well log of the

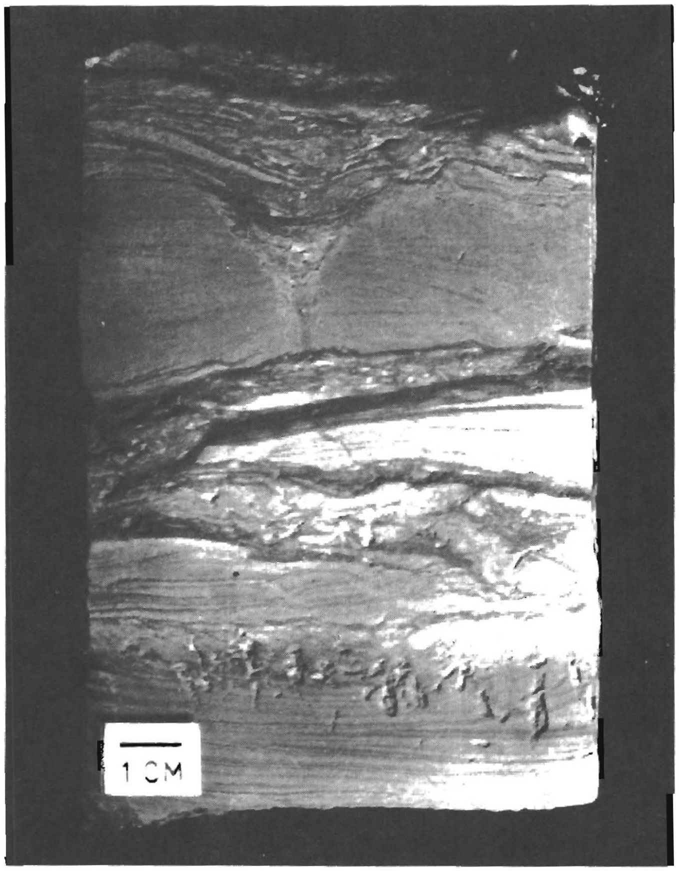

Figure 29. Core slab of a laminated and bioturbated mudstone. 5061.6 to 5061.2 feet.

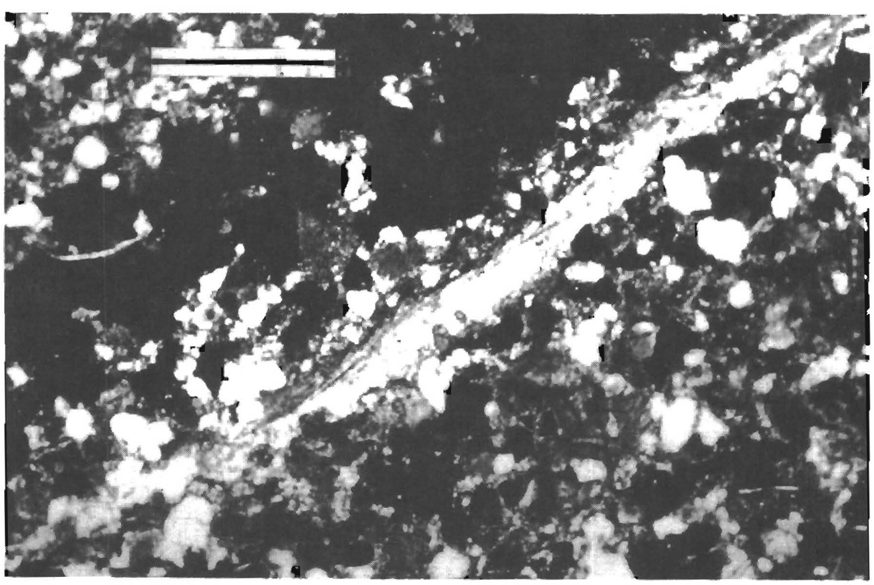

Figure 30. Photomicrograph of a fossiliferous quartzarenite. Stylolites rim the mollusk grain and quartz grains are penetrating the edges of the mollusk grain. Thin-section number 5020.5, 40X. Bar represents .5 mm.

Abrahamson #1-35 was used as the type well log for wells penetrating basal Swift carbonate bodies. This log was used because the interval in question had been cored, and a detailed correlation of the lithology and well-log character was possible.

The core confirms that the contact between the carbonate body and the underlying sediments is gradational over an interval of approximately 5 feet, and corresponds to the notable yet gradual change in the gamma-ray log and the resistivity log between 5,190 and 5,195 feet. The gradual coarsening-upward sequence from 5,190 to 5,086 feet is also recognized on the well log by the gradual decrease in the radioactivity readings and the increased resistivity readings.

The change from the packstone to the grainstone within the packstone-grainstone facies is also apparent on the log. This occurs at approximately 5,093 feet on the log and at 5,094 feet within the core.

The high resistivity readings throughout the carbonate body are related to the very low porosity of the packstone and the nature of the interstitial fluids within the available porosity of the grainstone. The reversed spontaneous-potential log indicates that the formation fluids of the grainstone were fresher than the drilling fluids within the hole. This is the reason for the high resistivity of this high-porosity zone.

The core shows that the upper contact of the carbonate body with the overlying shales is erosional. The increase in the gamma-ray log from 5,085 to 5,020 feet corresponds to the gradational change from the shale and mudstone, to the siltstone, and then to the quartzarenite. The interparticle porosity within the quartzarenite is denoted by the slight decrease in the resistivity readings between 5,040 and 5,030 feet. In thin section, the quartzarenite shows signs of compaction.

The well-log characteristics described above can be recognized on well logs of other wells penetrating basal Swift carbonates more than 25 feet thick. This thickness would result in more than just a single-spike, low gamma-ray-high resistivity log deflection. In the absence of other cores, the author believes that the physical characteristics seen in the Abrahamson core, and reflected in the logs for that well, can be applied to logs from other wells, which penetrate carbonate bodies.

Genesis of the Carbonate Bodies

Marine Environment

The environment of deposition of the carbonate bodies within the basal Swift Formation is believed to have been within the subtidal zone of a shallow marine shelf. A marine origin for the bodies is demonstrated by several lines of evidence. The abundance of marine fossils and the faunal assemblage present (Heckel, 1972) are indicative of a marine environment; however, it must be kept in mind that these fossil fragments have been transported.

The carbonate bodies are vertically enclosed in fine-grained sediments, which contain traces of marine fauna. It is inferred from the cross sections that the carbonate bodies interfinger with the surrounding shaly sediments. These shaly sediments exhibit similar well-log character on all sides of a carbonate body, indicating that a relatively uniform environment of deposition existed around the bodies.

The presence of glauconite has sometimes been suggested as a criterion for the recognition of normal marine environments (Cloud, 1955; Porrenga, 1967). McRae (1972, p. 413) disagrees with this and says that glauconite "is most commonly found in marine sediments," but that it has been found in non-marine environments. He suggests that glauconite is most often associated with marine transgressions. McRae (1972, p. 397) concludes that "the wide range of environmental conditions suitable for its formation and its common occurrence debars the use of glauconite in paleoenvironment studies."

Thin micritic rims surround almost all of the bioclastic grains within the packstone-grainstone facies. These rims are due to the boring of the outside of the shell fragments by algae (Bathurst, 1971, p. 90). Algae are confined to the photic zone, and are indicative of shallow marine waters.

Shallow Subtidal Zone

The actual depth of water involved in the deposition of the carbonate bodies is not known. Strong evidence points to the existence of shoaling conditions during the deposition of the carbonate sediments. This implies deposition near effective wave base. The well-rounded, well-sorted bioclastic grains throughout the packstone-grainstone facies indicate textural maturity, which is indicative of the reworking of the grains by waves and currents and the winnowing of the fines (Johnson, 1978).

The increase in grain size of the bioclasts from very fine grained at the base to coarse-grained at the top, suggests that the accumulation of the grains was upward into a gradually more turbulent environment (Exum, 1973; Rautman, 1978; Reinson, 1979). The gradual upward loss of micrite mud from between the grains and the loss of the very fine siliciclastic grains indicates apparent winnowing of the finer grain sizes as the sediment accumulated upward into a more turbulent water column. The imbricate grain orientation of the bioclasts within the carbonate body also suggests some transport (Reineck and Singh, 1980, p. 146).

Low-angle, parallel cross-laminations are a common feature in the deposits in shallow marine environments (Exum and Harms, 1968; Davies, 1969; Clifton, Hunter, and Phillips, 1971). These evenly laminated sands are abundant in high-energy beach environments and lower energy environments of submerged nearshore bars (Davidson-Arnott and Greenwood, 1974, 1976; Clifton, 1976). The bidirectional nature of the laminations indicates changes in flow direction across the body caused by wave and/or current activity. The presence of the apparent activation surfaces also indicates changes in flow conditions, renewed transport, and/or erosion (Harms and others, 1975).

Morphology

The approximate orientation and location of the carbonate bodies may be inferred from a paleofacies map constructed by Peterson (1957), and the thickness map of the carbonate bodies (pl. 2). According to Peterson (1957) and Carlson (1968), a marine glauconitic sand facies, located on a marine shelf, existed within the study area (fig. 31). The shoreline or basin margin was far to the east. The western edge of the study area marks the eastern edge of the deep-water facies (fig. 32). This suggests that the shelf margin or a notable change in the shelf slope occurred within the study area.

The thickness map of the carbonate bodies shows the general trend of the bodies in the area (pl. 2). Although the bodies are randomly scattered across the study area, they tend to lie parallel or at some small angle to the approximate paleoshoreline and the edge of the deep basin facies of Peterson (1957).

The geometry of these carbonate bodies is important in attempting to assess their origin. The carbonate bodies are randomly scattered across the area. The long axis of most of the bodies trends predominantly in a north-northeast to south-southwest, north-northwest to south-southeast direction with a secondary internal trend nearly perpendicular to this. The carbonate bodies farthest north in the study area have a more east-west orientation. In two areas of good well control, the dimensions of these bodies can be evaluated. These two areas extend from western Black Slough Field to eastern Rennie Lake Field and from the South Lonetree Field to southern Donnybrook Field. Respectively, the dimensions of the bodies range from 11 to 22 miles long, 4 to 7 miles wide, and 37 to 90 feet thick (pls. 2 and 3).

Possible Genetic Models

The morphology, composition, texture, and observed sedimentary structures of the marine, carbonate bodies suggests at least three possible models for their genesis: a shoreface model, a linear sand ridge model, and an offshore-bar model. Of these, the offshore-bar model appears to be most appropriate for the genesis of the Swift Formation carbonate bodies.

Offshore-Bar Model for the Genesis of the Carbonate Bodies

The basal Swift carbonates are randomly scattered across the study area. The carbonate bodies are usually elongate in a north-south direction, although the bodies in the northernmost part of the study area trend nearly east-west. The measured lengths and widths of the bodies depend in part on the availability of well control. In areas with moderate to

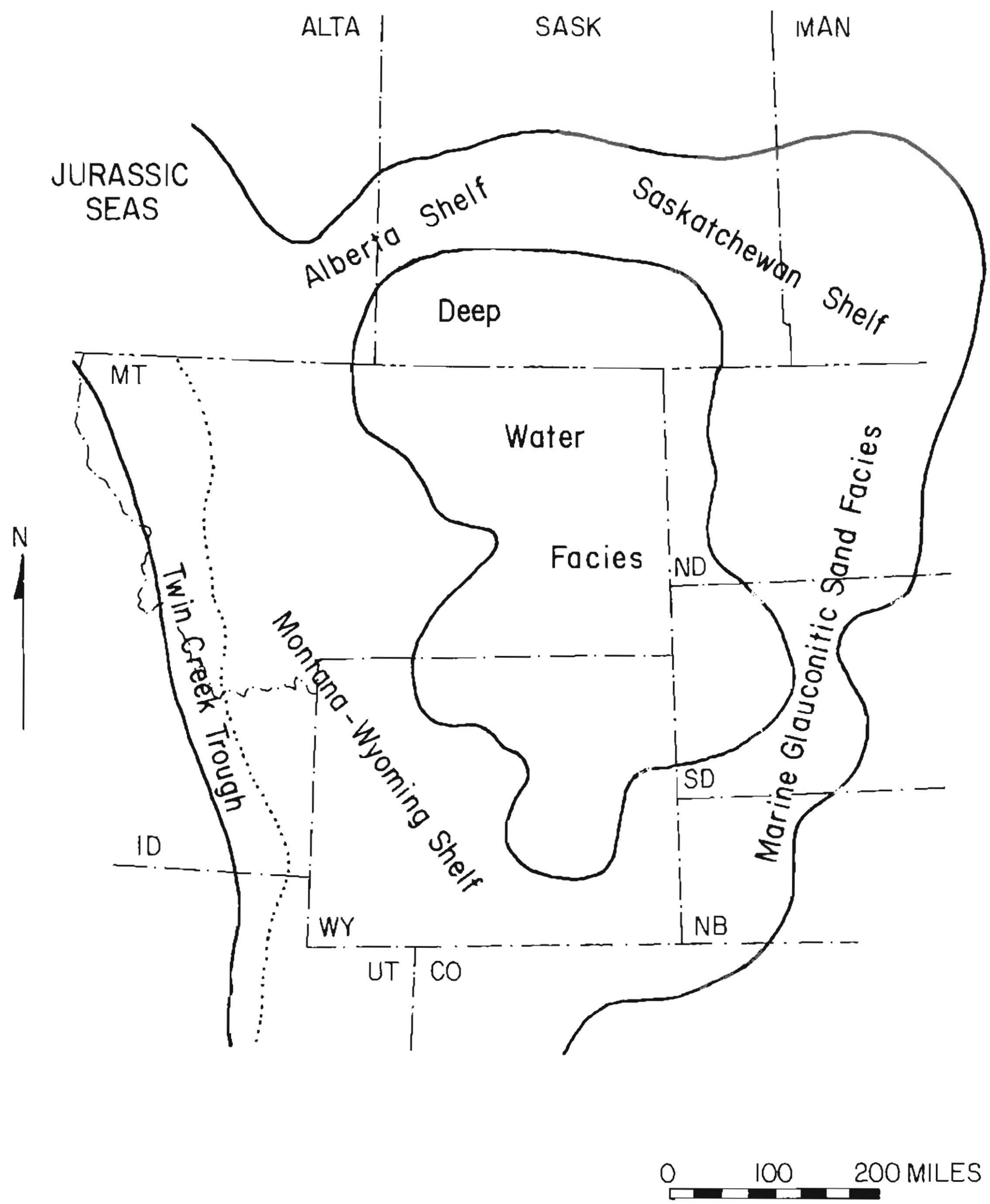

Figure 31. Generalized paleofacies map of the Northern Rocky Mountains and the Williston Basin (after Peterson, 1957, p. 432; Carlson, 1968).

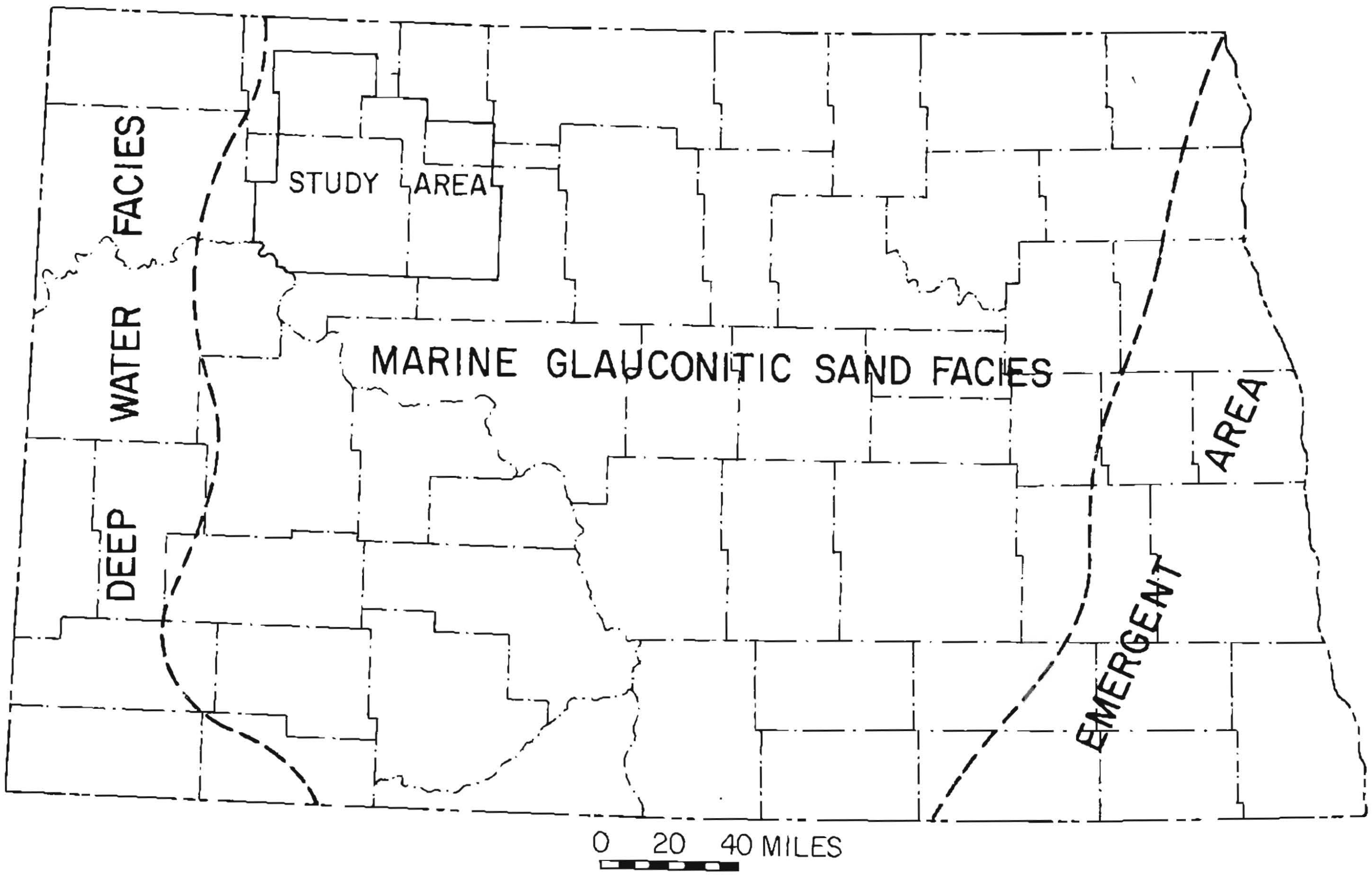

Figure 32. Area of study and its relationship to the paleofacies suggested by Peterson (1957, p. 432).

good well control, the bodies are 11 to 22 miles long, 4 to 7 miles wide, and 37 to 90 feet thick. The maximum thickness of the basal Swift carbonates penetrated is 155 feet.

Paleofacies and paleoenvironmental maps constructed by Peterson (1957) and by Carlson (1968) show the position of the edge of the Williston Basin extending slightly northeast to southwest across the eastern edge of North Dakota and the edge of the basin shelf occurring on the westernmost edge of Mountrail County (figs. 31 and 32). Considering the general trend of the carbonate bodies, this suggests that the carbonate bodies trend at a small acute angle, or almost parallel to the shoreline and shelf margin.

The relationship of the carbonate bodies to the relief on the underlying sediments at the time of deposition is unclear. Study of the isopach map of the Swift (pl. 1) reveals variations in the total thickness of the Swift. However, it is difficult to be certain whether these variations are the result of erosion of the upper surface of the Swift or due to differential dissolution of the underlying Dunham Salt (Salisbury, 1966) prior to deposition of the Swift. The stratigraphic cross sections do show some relief on the top of the Rierdon Formation. Some of this relief is reflected in unit A.

The basal Swift carbonate body represented by the Abrahamson #1-35 core is a coarsening-upward sequence composed of very fine to coarse-grained mollusk fragments. Minor quantities of echinoderm fragments, peloids, intraclasts, glauconite, and siliciclastic grains are present. The packstone portion of the packstone-grainstone facies is moderately to poorly sorted and contains well-rounded bioclastic grains and subangular to subrounded siliciclastic grains. The grainstone portion of this facies contains only well-rounded, well-sorted bioclastic material.

Low-angle, parallel cross-laminations are the most common sedimentary structures within the core. Dips on the cross-laminations are apparently bidirectional, and infrequent reactivation surfaces are recognized. Bioturbation is minor.

The character of the well logs and the cross sections indicates that the carbonate bodies are laterally and vertically surrounded by and interfingered with marine shales and shaly clastics. The core shows that the contact between the carbonate body and the underlying shaly, fine-grained, cross-laminated quartzarenite is gradational, whereas the upper contact is unconformable with the overlying marine shale. The base of this overlying shale contains clasts similar to the packstone of the underlying carbonate body.

If hummocky cross-laminations actually do occur, they probably suggest storm-generated waves and currents. Such laminations may indicate deposition of material from suspension after the passage of a wave generated by a storm (Harms and others, 1975). Recent studies have shown that some storms and their related currents can disturb sea floor sediments to depths greater than 325 feet and such storms can transport sands great distances across the shelf (Channon and Hamilton, 1976; Johnson, 1978). This supports the possibility of finding these structures in the offshore environment. No other evidence was found in either the core or the cross sections to suggest what processes or depth of water may have been involved in transporting the bioclastic material.

Three possible analogs have been described to explain the origin of the carbonate bodies. Two of the analogs, the shoreface model and the linear sand ridge model, are modern analogs. The third, the offshore bar, is derived from ancient sand bodies similar in stratigraphic occurrence and physical character. The vertical sequence of textures and sedimentary structures seen in the basal Swift carbonates resembles the sequence of structures that would be seen in a shoreface deposit, particularly the shoreface deposits of barred coasts such as barrier islands or nearshore bars (Davies and others, 1971; Dickinson and others, 1972; Davidson-Arnott and Greenwood, 1974, 1976). Although a case might be built for assigning the carbonate bodies to such an environment, it seems likely that, in light of what is known about the bodies and their surrounding sediments, that this is not the environment in which they formed. The carbonate bodies are not as clean or as well-sorted as shoreface deposits and they are much larger than any nearshore bar described in the literature. The studies of the Abrahamson core suggest that the

Abrahamson carbonate body was never emergent, as barrier islands or large nearshore bars would have been. No indication exists that non-marine or nearshore deposits such as dunes, lagoons, or deltas were ever present. It is possible, however, that any features in the carbonate body indicative of emergence were removed by erosion.

The carbonate bodies are also similar to linear sand ridges in their geometry, environment of deposition, and possibly in certain internal characteristics. Both the carbonate bodies and linear sand ridges are composed of sand-sized grains, both are characteristically elongate in a direction parallel to or at a small angle to the shoreline, and both may attain substantial thicknesses. Both types of deposits are found in the shallow marine environment and are surrounded by fines. Some linear sand ridges, thought to be storm-generated, show two internal features similar to the carbonate bodies: a coarsening-upward sequence (Duane and others, 1972; Stubblefield and others, 1975; Swift and Field, 1981) and hummocky cross-stratification (Harms and others, 1975; Walker, 1979).

However, certain major differences between linear sand ridges and the carbonate bodies do occur. Morphologically, the carbonate bodies lack the regular spacing and the well-oriented crests seen in the linear sand ridges, particularly those of tidal origin (Off, 1963; Houbolt, 1968).

The most notable differences between carbonate bodies and linear sand ridges are related to the basal contact and to the internal structures. The basal contact of a linear sand ridge is planar and unconformable; the unconformity is marked by the presence of a basal lag deposit that covers the sea floor (Houbolt, 1968; Swift and others, 1973). In contrast, the basal contact of the carbonate bodies is apparently undulatory and conformable with underlying sediments.

Internally, sand ridges may show no change, a fining-upward sediment sequence, or a coarsening-upward sequence of grain sizes (Houbolt, 1968; Stubblefield and others, 1975; Walker, 1979). The sands are most often clean and well sorted. Linear sand ridges apparently have large-scale, low-angle crossbedding (Ball, 1967; Houbolt, 1968). Bioturbation is also prominent in some linear sand ridges (Ball, 1967; Stubblefield and others, 1975).

The carbonate bodies within the study area have a consistent coarsening-upward character on the well logs and within the cored body. Small-scale, low-angle, cross-laminations and minor, trough, cross-laminations are prominent in the cored carbonate body of the basal Swift Formation. No large-scale features were observed.

The carbonate bodies studied within the basal Swift Formation are similar to certain ancient offshore bars that have been described elsewhere, particularly the marine bar described by Exum (1973). The sequence of textures and sedimentary structures present in all of the ancient offshore bars indicates gradual shoaling-water conditions. All of the ancient bars are surrounded by marine shales and fine-grained sediments.

The ancient offshore bars and the Swift carbonate bodies are morphologically similar. The bars and the bodies are slightly elliptical to elongate, relatively thick, irregularly spaced, and randomly located within the study area. Both the carbonate bodies and the ancient offshore bars become cleaner and are coarsening-upward sequences that are moderately poor to moderately well sorted.

The most common sedimentary structures seen in the core are the low-angle, parallel cross-laminations. Hummocky cross-laminations and small-scale trough cross-laminations may also be present.

It appears that the carbonate bodies of the Swift Formation have some characteristics similar to certain aspects of shoreface deposits and linear sand ridges, as well as to ancient offshore bars. The carbonate bodies may be a combination of the shoreface deposits and the linear sand ridges. The core has approximately the same sequence of internal sedimentary structures as the shoreface deposits, environmental setting, and morphology as the linear sand ridge. No single modern analog is known with these particular attributes. Only the ancient deposits described as offshore bars have internal characteristics, general morphology, and environmental setting similar to those of the basal Swift carbonate bodies.

The model proposed for the origin

of the carbonate bodies is similar to that suggested by Campbell (1971, 1973) and La Fon (1981) for similar deposits in the Upper Cretaceous of New Mexico. This model requires the transport of sediments across a shelf floor by bottom currents, which may be induced by storms, tides, or regional circulatory currents. Campbell (1971, 1973) suggests that a break in the slope of the shelf could initiate the deposition of the sediment in transport. Ball (1967) found that less than 10 feet of relief was sufficient to cause sands to concentrate on the edge of Florida Bay. Scanty evidence exists to suggest what currents or what direction of flow might have prevailed during the deposition of the Swift carbonate bodies. No information concerning the paleogeography of the area is available. Kumar and Sanders (1976) have suggested that plane parallel laminae will occur in high flow regimes associated with intense storms and that these will become cross-laminations as the storm subsides and the lower flow regime is entered. The presence of hummocky cross-laminations indicates storm-generated currents (Harms and others, 1975). The random occurrence of the carbonate bodies within the study area suggests some notable changes in current direction. Randomly oriented storm currents, rather than tidal currents, which assume more uniform flow paths, could be responsible for the apparently random occurrence of the Swift carbonate bodies. The limited access of the Jurassic seas to the main oceanic body would also decrease the possibility of generating tidal currents strong enough to act as the sole transporting agent of large amounts of sediment.

Evidence for slight local irregularities and changes in the slope of the lower Swift Formation can be found on the cross sections and by comparing the changes in thickness of the Swift Formation (pl. 1) and the thicknesses and occurrence of the carbonate bodies (pl. 2). This is particularly true around the Donnybrook to South Lonetree Field areas in the eastern part of the study area. Here it can be seen that the carbonate bodies are occurring where the Swift Formation is slightly thinner (< 400 feet), and that they are absent where the Swift Formation becomes noticeably thicker (> 400 feet). This might indicate a break in the slope of the shelf and deposition at that break.

Deposition of the Carbonate Bodies

Deposition of the carbonate bodies probably began during the final transgression of the Jurassic sea. This transgression occurred over a slightly irregular sea floor composed of shaly bottom sediments containing siliciclastic grains and bioclastic debris. Strong bottom currents, induced primarily by storm activity and enhanced by weak tidal currents and regional circulatory currents, began to interact with and transport sediments derived from the sea floor. These sediments were moved along the shelf until a slight break or irregularity occurred. The change in the slope probably caused current energies to decrease with the deepening of the water, and the decreased current energy initiated the deposition of the packstone portion of the carbonate body. This may explain the gradational contact between the packstone and the underlying fine-grained quartzarenites and the lateral interfingering with the surrounding sediments.

Deposition and progradation of the carbonate body apparently continued, gradually building upward into a higher energy regime. This resulted in the winnowing of the fines, the retention of the coarser grained sediments, and the development of the grainstone facies.

Cessation of the deposition of the carbonate bodies may have been due to decreased current activity, depletion of the source of the carbonate grains, increased basin subsidence and/or continued transgression of the seas. Continued transgression of the seas seems most probable because the carbonate bodies located in the north and northeast portion of the study area occur higher in the section than those to the south.

During or after the formation of these elongate calcarenite bodies, currents may have cut across them and developed features that resemble channels; these can be recognized on the thickness map of the carbonate bodies.

A period of non-deposition and erosion occurred before the deposition of the overlying shales. The initial deposition of the shales must have been under a low flow regime. Pebbles similar to the packstones within the underlying carbonate body occur within the lowest 4 inches of the shale indicating a brief period of higher flow. Continued deposition of the overlying sediments was under relatively quiet water conditions.

DEVELOPMENT OF MOLDIC POROSITY WITHIN THE PACKSTONE-GRAINSTONE FACIES

Moldic porosity is defined by Choquette and Pray (1970, p. 248) as porosity "formed by the selective removal, normally by solution, of a former individual constituent of sediment or rock such as a shell or oolith." Moldic porosity is a post-depositional feature and is a form of secondary porosity. This type of porosity is fabric-selective, indicating a direct relationship between the geometry and depositional position of the original grain (Choquette and Pray, 1970; Moore, 1979; Longman, 1981).

The development of moldic porosity is most commonly through the selective removal of grains composed of primary aragonite, such as mollusk grains, coral fragments, and ooliths (Dodd, 1966; Choquette and Pray, 1970; Longman, 1980; Moore and Druckman, 1981). The packstone-grainstone facies of the cored basal Swift carbonate body contains extensively infilled, partially infilled, and open molds of mollusk fragments. Preservation of the original particle shape, and subsequently the mold, was due to the presence of the micrite rim (Friedman, 1975). These infilled molds and the moldic porosity constitute one of the major diagenetic fabrics within the core.

The diagenetic fabric within the basal Swift carbonate bodies was produced by the dissolution of the abundant mollusk grains. The texture of the infilling cement strongly resembles that of the fresh-water phreatic zone. The molds within the packstone portion of the carbonate body are completely infilled with calcite cement. This infilling cement consists of either a faint, drusy rim cement and a coarse, subequant spar cement infilling the remaining pore, or a well-developed drusy cement rimming the grain with one or two anhedral calcite crystals infilling the pore.

The grainstone portion of the carbonate body has completely infilled molds similar to those in the packstone portion, molds containing a dog-tooth spar rim cement, and open molds. Similar, partially filled molds were found in the fresh-water phreatic zone of the Belmont Formation in Bermuda and were described by Land (1970).

The development of the moldic porosity within a fresh-water phreatic environment strongly suggests that the porosity within the core did not undergo extensive development until the formation of the post-Swift--pre-Inyan Kara unconformity. The fluvial deposits of the lower Inyan Kara Formation suggest a climate and environment capable of supplying notable quantities of meteoric water to the subsurface. The top of the basal Swift carbonate body lies within 300 feet of the unconformity and would undoubtedly have been within the limits of the fresh-water phreatic zone. The presence of predominantly siliciclastic sediments over the carbonate body would increase the chance that meteoric waters, undersaturated with calcium carbonate, would reach the body. The rate of fluid flow through the carbonate body is virtually impossible to evaluate, but the presence of open pores filled with relatively fresh water within grainstones suggests that the flow and exchange of fluids with the overlying sediments was sufficient to keep the pore waters from becoming saturated with calcium carbonate (reversed spontaneous-potential curve on the well log of the Abrahamson #1-35).

ECONOMIC POTENTIAL

No petroleum is produced from the carbonate bodies of the basal Swift Formation. The Upper Jurassic Roseray Formation (equivalent in age to the Swift Formation) of Saskatchewan is a well-sorted, fine-grained, poorly cemented quartzose sandstone, which produces low API gravity oil.

The requirements for the accumulation of hydrocarbons include: (1) a reservoir rock, with good porosity and permeability, (2) a trapping mechanism, and (3) a source for the hydrocarbons. The basal Swift carbonate bodies fulfill the first two requirements. The carbonate sands, particularly the grainstones, which are clean and maintain a relatively continuous composition and texture, are good reservoir rocks. They have a moldic porosity that ranges from 22 to 31 percent and a maximum permeability of 22 millidarcies (Terra Resources, Inc., Geologic Report on the Abrahamson #1-35, NDGS Well No. 6179). The porosity and permeability of the packstones is notably less. The elongate and concave shape of the bodies surrounded by impervious sediments, provide a good trapping mechanism.

The third requirement, a hydrocarbon source, is the critical factor. The amount of organic matter that would have remained after significant transport and abrasion of the shell material is unknown, but it is unlikely that significant amounts would have been left. Therefore, oil or gas generation from within the body itself seems doubtful.

The surrounding shales may be potential source rocks, but their shallow depths (approximately 5,000 feet) suggest that the temperatures appropriate for substantial oil generation did not occur. Oil migration from thermally mature sources underlying the Swift Formation must also be considered, but this possibility is still speculative.

The possibility exists that biogenic gas, derived from the surrounding shales, could be present within the grainstones. Biogenic gas is generated at low temperatures and at relatively shallow depths by the decomposition of organic matter by anaerobic microorganisms. Such gas could have formed even though the shales were not deeply buried and did not undergo the high temperatures and pressures required for oil generation.

CONCLUSIONS

Examination of approximately 680 mechanical well logs along with the one available core from the Terra Resources, Inc., Abrahamson #1-35 test hole has shown that the carbonate bodies within the basal Swift Formation may be packstones and grainstones composed of predominantly sand-sized, well-rounded, recrystallized mollusk fragments as found in the Abrahamson core. The carbonate sand bodies are located in various stratigraphic positions within the lower 150 feet of the Swift Formation. They variably replace units A, B, and C of the Swift Formation. The basal contact of the bodies is conformable with the underlying sediments; the upper contact is unconformable and marked by a break from carbonate sand to shale. Lateral changes occur through the interfingering of the carbonate sands with the surrounding shales and very fine clastics. The sand bodies are randomly scattered throughout the study area, but their long axes tend to be oriented parallel or sub-parallel to what would have been the paleoshoreline of the Williston Basin during Swift (Oxfordian) time.

Comparison of the sedimentary structures, textures, and morphology of the carbonate sand bodies with modern and ancient analogs suggests that the bodies are large offshore sand bars that were deposited during the final transgression of the shallow epicontinental sea across the irregular shelf floor of the eastern Williston Basin. The bodies were apparently generated when strong bottom currents (current direction unknown), moving across the irregular shelf floor, encountered local breaks in the shelf, resulting in deposition of the carbonate sands where the bottom currents slowed due to deepening of the water.

Continued transport and deposition of the bioclastic debris caused the offshore bars to prograde laterally and vertically. This progradation resulted in the lateral interfingering of the carbonate sands with the surrounding shales and very fine clastics. The vertical accumulation of the bars resulted in a coarsening-upward sequence of carbonate sands that attained thicknesses greater than 100 feet in several areas.

Shales were deposited over the carbonate bodies as the Jurassic seas transgressed and became deeper. Deposition of the shales was followed by the deposition of coarser clastics (siltstones and quartzarenites). The well-log character suggests that these clastics occur throughout the upper Swift Formation and are probably related to the gradual retreat of the marine interior seas. Final retreat of the seas was followed by post-Swift, pre-Inyan Kara erosion.

The shallow burial of the carbonate sand bodies, the presence of the aragonitic mollusk grains, and the presence of a fresh-water phreatic zone fed by the fluvial systems of the Early Cretaceous provided optimum conditions for the development of the infilled molds and the moldic porosity found within the carbonate sand bodies.

The carbonate bodies have the necessary characteristics of good reservoir rock, but they lack the presence of a mature hydrocarbon source. These bodies may have the potential for the accumulation of biogenic gas derived from the surrounding shales, and, therefore, could be good sites for potential exploration.

REFERENCES

Anderson, S. B., 1964, Salt deposits of North Dakota, in Tufte, O. (ed.), Mineral Resources of North Dakota: North Dakota Economic Development Commission, University of North Dakota, Grand Forks, North Dakota, p. 60-79.

Ball, M. M., 1967, Carbonate sand bodies of Florida and the Bahamas: Journal of Sedimentary Petrology, v. 37, no. 2, p. 556-591.

Bathurst, R. G. C., 1971, Carbonate Sediments and their Diagenesis, Developments in Sedimentology 12: New York, Elsevier Scientific Publishing Company, 658 p.

Bluemle, J. P., Anderson, S. B., and Carlson, C. G., 1980, North Dakota Stratigraphic Column: North Dakota Geological Survey.

Bluemle, J. P., Anderson, S. B., and Carlson, C. G., 1981, Williston Basin Stratigraphic Nomenclature Chart: North Dakota Geological Survey Miscellaneous Series 61.

Brook, Margaret, and Braun, W. K., 1972, Biostratigraphy and microfaunas of the Jurassic System of Saskatchewan: Department of Mineral Resources, Geological Science Branch Report 161, 83 p.

Campbell, C. V., 1971, Depositional model--Upper Cretaceous Gallup beach shoreline, Ship Rock area, northwestern New Mexico: Journal of Sedimentary Petrology, v. 41, no. 2, p. 395-409.

Campbell, C. V., 1973, Offshore equivalents of Upper Cretaceous Gallup beach sandstone, northwestern New Mexico, in Fasset, J. E. (ed.), Cretaceous and Tertiary rocks of the southern Colorado Plateau: Four Corners Geological Society Memoir, p. 78-84.

Carlson, C. E., 1968, Triassic-Jurassic of Alberta, Saskatchewan, Manitoba, Montana, and North Dakota: American Association of Petroleum Geologists Bulletin, v. 52, no. 10, p. 1969-1983.

Carlson, C. G., and Anderson, S. B., 1965, Sedimentary and Tectonic History of North Dakota Part of Williston Basin: American Association of Petroleum Geologists Bulletin, v. 49, no. 11, p. 1833-1846.

Channon, W. A., and Hamilton, 1976, Wave and tidal current sorting of shelf sediments southwest of England: Sedimentology, v. 23, p. 17-42.

Choquette, P. W., and Pray, L. C., 1970, Geologic nomenclature and classification of porosity in sedimentary carbonates: American Association of Petroleum Geologists Bulletin, v. 54, no. 2, p. 207-250.

Clifton, H. E., 1976, Wave-formed sedimentary structures - a conceptual model, in Beach and Nearshore Sedimentation, Davis, Richard, Jr., and Ethington, R. L. (eds.), Society of Economic Paleontologists and Mineralogists Special Publication 24, p. 126-148.

Clifton, H. E., Hunter, R. E., and Phillips, R. L., 1971, Depositional structures and processes in the non-barred high energy nearshore: Journal of Sedimentary Petrology, v. 41, p. 651-670.

Cloud, P. E., Jr., 1955, Physical limits of glauconite formation: American Association of Petroleum Geologists Bulletin, v. 39, no. 4, p. 484-492.

Cobban, W. A., 1945, Marine Jurassic formations of Sweetgrass Arch, Montana: American Association of Petroleum Geologists Bulletin, v. 29, no. 9, p. 1262-1303.

Davidson-Arnott, R. G. D., and Greenwood, B., 1974, Bedforms and structures associated with bar topography in the shallow water wave environment, Kouchibouguac Bay, New Brunswick, Canada: Journal of Sedimentary Petrology, v. 44, no. 3, p. 698-704.

Davidson-Arnott, R. G. D., and Greenwood, B., 1976, Facies relationships on a barred coast, Kouchibouguac Bay, New Brunswick, Canada, in Davis, R. A., Jr., and Ethington, R. L. (eds.), Beach and Nearshore Sedimentation: Society of Economic Paleontologists and Mineralogists Special Publication 24, p. 149-168.

Davies, D. K., 1969, Shelf sedimentation: an example from the Jurassic of Britain: Journal of Sedimentary Petrology, v. 39, no. 4, p. 1344-1370.

Davies, D. K., Ethridge, F. G., and Berg, R. R., 1971, Recognition of barrier environments: American Association of Petroleum Geologists Bulletin, v. 55, no. 4, p. 550-565.

Dickinson, K. A., Berryhill, H. L., and Holmes, C. W., 1972, Recognizing ancient barrier coastlines, in Rigby, J. K., and Hamblin, Wm. K. (eds.), Recognition of Ancient Sedimentary Environments: Society of Economic Paleontologists and Mineralogists Special Publication 16, p. 192-214.

Dodd, J. R., 1966, Process of conversion of aragonite to calcite with examples from the Cretaceous of Texas: Journal of Sedimentary Petrology, v. 36, no. 3, p. 733-741.

Duane, D. B., Field, M. E., Meisburger, E. P., Swift, D., and Williams, S. J., 1972, Linear shoals on the Atlantic Inner Continental Shelf, Florida to Long Island, in Swift, D., Duane, D. B., and Pilkey, Orrin (eds.), Shelf Sediment Transport: Stroudsburg, Dowden, Hutchison, and Ross, Inc., p. 447-498.

Dunham, R. J., 1962, Classification of carbonate rocks according to depositional texture, in Ham, W. E. (ed.), Classification of Carbonate Rocks: American Association of Petroleum Geologists Memoir 1, p. 108-121.

Exum, F. A., 1973, Lithologic gradients in marine bar, Cadeville sand, Calhoun field, Louisiana: American Association of Petroleum Geologists Bulletin, v. 57, no. 2, p. 301-320.

Exum, F. A., and Harms, J. C., 1968, Comparison of marine-bar with valley-fill stratigraphic traps, western Nebraska: American Association of Petroleum Geologists Bulletin, v. 52, no. 10, p. 1851-1868.

Folk, R. L., 1965, Some aspects of recrystallization in ancient limestones, in Friedman, G. M., and Ali, S. A. (eds.), Diagenesis of Carbonate Rocks: Cement Porosity Relationships: Society of Economic Paleontologists and Mineralogists Reprint Series 10, p. 28-62.

Folk, R. L., 1974, Petrology of Sedimentary Rocks: Austin, Hemphill Publishing Company, 182 p.

Francis, D. R., 1956, Jurassic stratigraphy of the Williston Basin area: Saskatchewan Department of Mineral Resources, Geological Sciences Branch Report 18, 69 p.

Friedman, G. M., 1959, Identification of carbonate minerals by staining methods: Journal of Sedimentary Petrology, v. 29, no. 1, p. 87-97.

Friedman, G. M., 1975, The making and unmaking of limestones or the ups and downs of porosity: Journal of Sedimentary Petrology, v. 45, no. 2, p. 379-398.

Harms, J. C., Southard, J. B., Spaering, D. R., and Walker, R. G., 1975, Depositional Environments as Interpreted from Primary Sedimentary Structures and Stratification Sequences: Tulsa, Society of Economic Paleontologists and Mineralogists Short Course 2, 161 p.

Heckel, Phillip, 1972, Recognition of ancient shallow marine environments, in Rigby, J. Keith (ed.), Recognition of Ancient Sedimentary Environments: Society of Economic Paleontologists and Mineralogists Special Publication 16, p. 226-286.

Houbolt, J. J. H. C., 1968, Recent sediments in the southern bight of the North Sea: Geologie En Mijnbouw, v. 47, no. 4, p. 245-273.

Hunter, R. E., and Clifton, H. E., 1982, Cyclic deposits and hummocky cross-stratification of probable storm origin in Upper Cretaceous rocks of the Cape Sebastian area, southwestern Oregon: Journal of Sedimentary Petrology, v. 52, no. 1, p. 127-144.

Illing, L. V., 1954, Bahamian calcareous sands: American Association of Petroleum Geologists Bulletin, v. 38, no. 1, p. 1-95.

Imlay, R. W., 1947, Marine Jurassic of Black Hills area, South Dakota and Wyoming: American Association of Petroleum Geologists Bulletin, v. 31, no. 2, p. 227-273.

Imlay, R. W., 1980, Jurassic paleobiogeography of the conterminous United States in its continental setting: United States Geological Survey Professional Paper 1062, 134 p.

Imlay, R. W., Gardner, L. S., Rogers, C. P., and Hadley, H. D., 1948, Marine Jurassic formations of Montana: United States Geological Survey Oil and Gas Investigation Preliminary Chart 32.

Johnson, H. D., 1978, Shallow siliciclastic seas, in Reading, H. G. (ed.), Sedimentary Environments and Facies: New York, Blackwell Scientific Publications, p. 207-258.

Kumar, Naresh, and Sanders, J. E., 1976, Characteristics of shoreface storm deposits: modern and ancient examples: Journal of Sedimentary Petrology, v. 46, no. 1, p. 145-162.

Laird, W. M., and Towse, D. F., 1953, Stratigraphy of North Dakota with reference to oil possibilities: North Dakota Geological Survey Report of Investigation 2 (revised), 2 sheets.

Land, L. S., 1970, Phreatic versus vadose meteoric diagenesis of limestones: evidence from a fossil water table: Sedimentology, v. 14, p. 175-185.

La Fon, N. A., 1981, Offshore bar deposits of Semilla Sandstone member of Mancos Shale (Upper Cretaceous), San Juan Basin, New Mexico: American Association of Petroleum Geologists Bulletin, v. 65, no. 4, p. 706-721.

Longman, M. W., 1980, Carbonate diagenetic textures from nearshore diagenetic environments: American Association of Petroleum Geologists Bulletin, v. 64, no. 4, p. 461-487.

Longman, M. W., 1981, Carbonate diagenesis and hydrocarbon exploration: unpublished manuscript, 58 p.

McRae, S. G., 1972, Glauconite: Earth Science Review, v. 8, p. 397-440.

Milner, R. L., and Thomas, G. E., 1954, Jurassic System in Saskatchewan, in Clark, L. M. (ed.), Western Canada Sedimentary Basin--Ralph Leslie Rutherford Memorial Volume: American Association of Petroleum Geologists, p. 250-267.

Milner, R. L., and Blakslee, G. W., 1958, Notes of the Jurassic of southwestern Saskatchewan, in Goodman, A. J. (ed.), Jurassic Carboniferous of Western Canada--John Andrew Allan Memorial Volume: American Association of Petroleum Geologists, p. 65-84.

Moore, C. H., 1979, Porosity in carbonate rock sequences, in Geology of Carbonate Porosity: American Association of Petroleum Geologists Course Note Series 11, p. A1-A124.

Moore, C. H., and Druckman, Yehezkeel, 1981, Burial diagenesis and porosity evolution Upper Jurassic Smackover, Arkansas and Louisiana: American Association of Petroleum Geologists Bulletin, v. 65, no. 4, p. 597-628.

Nordquist, J. W., 1955, Pre-Rierdon Jurassic stratigraphy in northern Montana and Williston Basin: in Sixth Annual Field Conference, Sweetgrass Arch-Disturbed Belt, Montana, Billings Geological Society, p. 96-106.

Off, Theodore, 1963, Rhythmic linear sand bodies caused by tidal currents: American Association of Petroleum Geologists Bulletin, v. 47, no. 2, p. 324-341.

Peterson, J. A., 1957, Marine Jurassic of northern Rocky Mountains and Williston Basin: American Association of Petroleum Geologists Bulletin, v. 41, no. 3, p. 399-440.

Peterson, J. A., 1958, Paleotectonic control of marine Jurassic sedimentation in the Powder River Basin: in Thirteenth Annual Field Conference, Powder River Basin, Wyoming Geological Society, p. 56-63.

Porrenga, O. H., 1967, Glauconite and chamosite as depth indicators in the marine environment: Marine Geology, v. 5, p. 495-501.

Purdy, E. G., 1968, Carbonate diagenesis: an environmental survey: Geologic Romana, v. 7, p. 183-228.

Rautman, C. A., 1978, Sedimentology of Late Jurassic barrier island complex--Lower Sundance Formation of the Black Hills: American Association of Petroleum Geologists Bulletin, v. 62, no. 11, p. 2275-2289.

Reineck, H. E., and Singh, I. B., 1980, Depositional Sedimentary Environments, with References to Terrigenous Clastics: New York, Springer-Verlag, 549 p.

Reinson, G. E., 1979, Barrier island systems, in Walker, R. G. (ed.), Facies Models: Geoscience Canada Reprint Series 1, p. 57-74.

Salisbury, R. A., 1966, Jurassic stratigraphy of the southern two-thirds of North Dakota: University of North Dakota, Grand Forks, unpublished Master of Science thesis, 124 p.

Stott, D. F., 1955, Jurassic stratigraphy of Manitoba: Manitoba Department of Mines and Natural Resources Publication 54-2, 78 p.

Stubblefield, W. L., Lavelle, J. W., Swift, D. J. P., and McKinney, T. J., 1975, Sediment response to the present hydraulic regime on the central New Jersey shelf: Journal of Sedimentary Petrology, v. 45, no. 1, p. 337-358.

Swift, D. J. P., Duane, D. B., and McKinney, T. F., 1973, Ridge and swale topography of the Middle Atlantic Bight, North America: secular response to the Holocene hydraulic regime: Marine Geology, v. 15, p. 227-247.

Swift, D. J. P., and Field, M. E., 1981, Evolution of a classic sand ridge field: Maryland sector, North American Inner shelf: Sedimentology, v. 28, no. 4, p. 461-482.

Walker, R. G., 1979, Shallow marine sands, in Walker, R. G. (ed.), Facies Models: Geoscience Canada Reprint Series 1, p. 75-90.

APPENDIX A

CORE DESCRIPTION WITH THIN-SECTION LOCATIONS

APPENDIX A

CORE DESCRIPTION WITH THIN-SECTION LOCATIONS

The following description is of the core taken from the Terra Resources, Inc., Abrahamson #1-35, NDGS Well No. 6179. The description is by 1-foot intervals from stratigraphically highest to lowest depth. Locations of thin sections and their assigned name are listed by depth, from stratigraphically highest to lowest position. The carbonates are named according to Dunham's (1962) classification, and the siliciclastics are named according to Folk's (1974) classification. Description format is texture, sedimentary structures, and diagenetic features. In cases where only minor variations occurred "same above" was used and the variation or addition was added to the end.

Depth	T.S.	Description
5020-5021		Quartzarenite: light-gray-green, fine-grained, subangular, moderately well sorted; calcareous; very silty molluscan-echinoderm hash; glauconitic; massive; interparticle porosity
	5020.5	Quartzarenite
5021-5022		Quartzarenite: same above; slightly laminated, bioturbated
5022-5023		Quartzarenite: same above; minor shale partings, not bioturbated
5023-5024		Quartzarenite: same above; interlaminated shales, bioturbated
	5023.1	Quartzarenite
5024-5025		Shale: green-gray; waxy, non-calcareous; calcareous siltstone laminations; bioturbated
5025-5026		Quartzarenite: light-gray-green, subangular, moderately well sorted; calcareous; glauconite-pyrite prominent; bioturbated; green shale laminations
5026-5027		Quartzarenite: light-gray-green, very fine grained, moderately well sorted; calcareous; glauconite, pyrite; bioturbated; green shale partings; interparticle porosity
	5026.4	Quartzarenite: bioturbated; calcareous
5027-5028		Quartzarenite: same above
	5027.7	Quartzarenite: very fine to fine-grained; mottled; calcareous
	5027.9	Quartzarenite: same above
5028-5029		Quartzarenite: shale laminations
	5028.7	Quartzarenite: same above, bioturbated
5029-5030		Quartzarenite: light-gray-green; very fine to fine-grained, subangular, well-sorted; calcareous; glauconite; siltstone-green shale partings; interparticle porosity
5030-5031		Quartzarenite: same above

Depth	T.S.	Description
5031-5032		Quartzarenite: same above; cross-laminations, ripples, bioturbated (?)
	5031.2	Quartzarenite: laminated
	5031.5	Quartzarenite: ripples
	5031.7	Quartzarenite: bioturbated
5032-5033		Quartzarenite: same above
5033-5034		Quartzarenite: same above
	5033.7TV	Quartzarenite
	5033.8	Quartzarenite
5034-5035		Quartzarenite: same above
5035-5036		Quartzarenite: same above
5036-5037		Quartzarenite: same above
	5037.0	Quartzarenite
5037-5038		Quartzarenite: same above; parallel laminations, cross-trough laminations
5038-5039		Quartzarenite: light-gray-green, very fine grained, subangular, moderately well sorted; calcareous; glauconite; siltstone-green shale partings, bioturbated; interparticle porosity
5039-5040		Quartzarenite: same above
5040-5041		Siltstone: same above; very fine sand; few cross-trough laminations
5041-5042		Siltstone: same above
	5041.6	Siltstone: laminated, glauconite, poorly sorted
5042-5043		Siltstone: same above; parallel and cross-trough laminations, very silty
	5042.7	Siltstone: very silty
5043-5044		Siltstone: light-gray-green, subangular, moderately well sorted; calcareous; very sandy; micaceous, glauconite; green shale laminations prominent; bioturbated
	5043.7	Siltstone
5044-5045		Siltstone: same above; shale abundant
5045-5046		Siltstone: same above
5047-5048		Siltstone: same above; shale abundant
5048-5049		Siltstone: same above

Depth	T.S.	Description
5049-5050		Siltstone: same above; little-to-no sand
5050-5051		Siltstone: same above; no sand
5051-5052		Siltstone: same above; no sand
5052-5053		Siltstone: green subangular, moderately well sorted; calcareous; very shaly (non-calcareous), micaceous, glauconite; laminated; bioturbated
5053-5054		Siltstone: same above; interlaminated with green shale
5054-5055		Siltstone: same above
5055-5056		Siltstone and Shale: light-green-gray, laminated, bioturbated siltstone: subangular, poorly sorted; slightly calcareous; glauconite shale: waxy, fissile; very slightly calcareous; slightly micaceous
5056-5057		Siltstone and Shale: same above
5057-5058		Siltstone and Shale: same above
5058-5059		Mudstone: dark-green; waxy; fissile; slightly calcareous; very silty; siltstone laminations; bioturbated; swelling green clays
	5059	Mudstone: very silty
5059-5060		Mudstone: same above; slight decrease in silt
5060-5061		Mudstone: same above
5061-5062		Mudstone: same above; highly bioturbated
5062-5063		Mudstone: same above; minor intraclasts
5063-5064		Mudstone: same above; highly bioturbated
5064-5065		Mudstone: same above
5065-5066		Mudstone: same above
5066-5067		Mudstone: same above; cross-laminated
	5066.3	
5067-5068		Mudstone: same above
5068-5069		Mudstone: same above
5069-5070		Mudstone: same above
5070-5071		Mudstone: same above
5071-5072		Mudstone: dark-green, waxy, fissile; slightly calcareous; very silty; siltstone laminations, bioturbated; swelling green clays
	5071.1	Mudstone

Depth	T.S.	Description
5072-5073		Mudstone: same above
5073-5074		Mudstone: same above
5074-5075		Mudstone: same above
	5074.9	Mudstone
5075-5076		Mudstone: same above
5076-5077		Shale: dark-green, waxy, fissile; slightly calcareous; silty, bioturbated; swelling green clays
5077-5078		Shale: same above
5078-5079		Shale: same above
5079-5080		Shale: same above
5080-5081		Shale: same above
5081-5082		Shale: same above
5082-5083		Shale: same above
5083-5084		Shale: same above
5084-5085		Shale: same above
5085-5086		Shale: dark-green, waxy, fissile; very slightly calcareous; slightly silty, swelling green clays, siltstone laminations; thinly laminated, bioturbated; rip-up clasts of light-gray packstone
5086-5087		Grainstone: gray-tan; medium- to fine-grained; moderately well sorted; partially leached molluscan-echinoderm grains, intraclasts, superficial oolites; sparry calcite, trace anhydrite (?) and dolomite; moldic porosity (20%-25%)
	5086.3	Recrystallized Molluscan Grainstone
	5086.4	Recrystallized Molluscan Grainstone
5087-5088		Grainstone: same above; stylolites
5088-5089		Grainstone: same above
	5088.7	Recrystallized Molluscan Grainstone
5089-5090		Grainstone: same above
5090-5091		Grainstone: same above
	5090.6	Recrystallized Molluscan Grainstone
5091-5092		Packstone-Grainstone
	5091.3	Recrystallized Molluscan Packstone-Grainstone
	5091.4	Recrystallized Molluscan Packstone-Grainstone

Depth	T.S.	Description
5092-5093		Packstone-Grainstone
5093-5094		Grainstone-Packstone
	5093.9	Recrystallized Molluscan Grainstone-Packstone
	5093.9TV	Recrystallized Molluscan Grainstone-Packstone
5094-5095		Packstone: gray to tan, medium to fine bioclasts, well-rounded, moderately well sorted; recrystallized molluscan-echinoderm grains, peloids, intraclasts, superficial oolites; stringers silt and sand; opaques; infilled moldic porosity
	5094.0	Recrystallized Molluscan Packstone
	5095.0	Recrystallized Molluscan Packstone
5095-5096		Packstone: same above; very fine sand and silt in matrix, stylolites, calcite-filled fracture, opaques
	5096.7	Recrystallized Molluscan Packstone
5096-5097		Packstone: same above; stylolites
	5097.1	Recrystallized Molluscan Packstone
5097-5098		Packstone: same above; stylolite, very silty, laminated, glauconite
	5097.1	Recrystallized Molluscan Packstone
5098-5099		Packstone: light-gray to green, medium to coarse bioclasts, moderately well sorted; spar calcite; recrystallized molluscan-echinoderm grains, peloids, intraclasts, superficial oolites, oolites; silt, very fine sand, glauconite, opaques; thinly laminated silts and sands; solution fractures, stylolites; infilled moldic porosity
	5099.0	Recrystallized Molluscan Packstone
5099-5100		Packstone: same above
5100-5101		Packstone: same above
5101-5102		Packstone: same above
5102-5103		Packstone: same above
5103-5104		Packstone: same above; massive
5104-5105		Packstone: same above; very fine sand laminations
5105-5106		Packstone: same above
5106-5107		Packstone: same above
	5106.5	Recrystallized Molluscan Packstone: sollution cavity prominent
5107-5108		Packstone: same above
5108-5109		Packstone: same above

Depth	T.S.	Description
5109-5110		Packstone: same above; inclined, thinly laminated, very fine sand prominent
	5109.7	Recrystallized Molluscan Packstone: laminated
	5109.8TV	Recrystallized Molluscan Packstone
5110-5111		Packstone: same above
5111-5112		Packstone: same above
	5112.0	Recrystallized Molluscan Packstone
5112-5113		Packstone: same above
5113-5114		Packstone: same above; minor silt and sand in matrix
5114-5115		Packstone: same above; large cavity filled with spar calcite, silt, fossiliferous
	5115.8	Recrystallized Molluscan Packstone
	5115.9TV	Recrystallized Molluscan Packstone
5116-5117		Packstone: light-gray to green, medium to coarse bioclasts, moderately well sorted; spar calcite; recrystallized molluscan-echinoderm grains, peloids, intraclasts, superficial oolites; silt and very fine sand, glauconite, opaques; inclined, thinly laminated silts and sands, stylolites, solution fractures occasionally
	5116.3	Recrystallized Molluscan Packstone
5117-5118		Packstone: same above; stylolites
	5118.0	Recrystallized Molluscan Packstone
5118-5119		Packstone: same above; stylolites, waxy green shale intraclasts
5119-5120		Packstone: same above; waxy green shale intraclasts, peloidal material prominent
5120-5121		Packstone: same above; sudden reversal in direction of inclination on laminations, stylolite
5121-5122		Packstone: light-gray to green, fine to medium bioclasts, moderately well sorted; spar calcite; recrystallized molluscan-echinoderm grains, peloids, intraclasts, superficial oolites; glauconite, opaques, very fine sand, silt in matrix; frequently laminated with silts and fine sands, stylolites; infilled moldic porosity
	5121.6	Recrystallized Molluscan Packstone
5122-5123		Packstone: same above
5123-5124		Packstone: same above
5124-5125		Packstone: same above

Depth	T.S.	Description
5125-5126		Packstone: same above; stylolites
5126-5127		Packstone: same above; trace waxy green shale clasts, solution fracture and cavity infilled with spar calcite silt and very fine grained sand
5127-5128		Packstone: same above
	5127.2	Recrystallized Molluscan Packstone
	5127.3	Recrystallized Molluscan Packstone
5128-5129		Packstone: same above; stylolites, solution fractures
5129-5130		Packstone: same above; soft sediment deformation (?)
5130-5131		Packstone: same above; medium bioclasts predominant; inclined parallel laminations, increasing laminations of fine sand
5131-5132		Packstone: same above; solution cavities filled with sparry calcite
5132-5133		Packstone: same above; solution fractures filled with sparry calcite
5133-5134		Packstone: same above
5134-5135		Packstone: same above
	5134.4	Recrystallized Molluscan Packstone
5135-5136		Packstone: light-gray to green-tan, fine- to medium-grained, moderately well sorted; sparry calcite; recrystallized molluscan-echinoderm grains, peloids, oolites, superficial oolites; glauconite, silt, and very fine sand in matrix; laminated with very fine sands and silts; stylolites, solution fractures, and cavities; infilled moldic porosity
	5135.1	Recrystallized Molluscan Packstone
	5135.4TV	Recrystallized Molluscan Packstone
5136-5137		Packstone: same above, stylolites
	5136.6	Recrystallized Molluscan Packstone
5137-5138		Packstone: same above; opaques, very thinly cross-laminated
5138-5139		Packstone: same above; stylolites
	5138.6	Recrystallized Molluscan Packstone
5139-5140		Packstone: same above; fine- to medium-sand stringers
	5139.5	Recrystallized Molluscan Packstone
5140-5141		Packstone: same above; solution fractures filled with sparry calcite
5141-5142		Packstone: same above

Depth	T.S.	Description
5142-5143		Packstone: same above; opaques
5143-5144		Packstone: same above; sudden change in direction of inclined laminations
	5144.0	Recrystallized Molluscan Packstone
5144-5145		Packstone: same above; solution fractures and cavities infilled with spar calcite, stylolites
	5144.3	Recrystallized Molluscan Packstone
5145-5146		Packstone: same above; stylolites, inclined parallel laminations
5146-5147		Packstone: same above; change in direction of inclination on parallel laminations
5147-5148		Packstone: same above
5148-5149		Packstone: same above; stylolites
	5148.8	Recrystallized Molluscan Packstone
5149-5150		Packstone: same above; stylolites, opaques
5150-5151		Packstone: light-green-gray, medium to coarse bioclasts, moderately well sorted; sparry calcite; recrystallized molluscan-echinoderm grains, peloids, intraclasts, superficial oolites, oolites; silt and very fine sand in matrix, glauconite, opaques; occasional silt and sand laminations; stylolites, infilled moldic porosity
5151-5152		Packstone: same above
5152-5153		Packstone: same above; solution fractures infilled with calcite, change in inclination of laminations
5153-5154		Packstone: same above
	5153.5TV	Recrystallized Molluscan Packstone
5154-5155		Packstone: same above; stylolites, solution fractures infilled with calcite, prominent 5-10° dip of laminations
5155-5156		Packstone: same above; opaques, finely laminated
5156-5157		Packstone: same above; prominent glauconitic sand stringer, 10° dip of laminations, solution fractures infilled with calcite
	5157.0	Recrystallized Molluscan Packstone
5157-5158		Packstone: same above; stylolites
5158-5159		Packstone: same above
5159-5160		Packstone: same above; stylolites, solution fracture infilled with calcite
	5159.1	Recrystallized Molluscan Packstone

Depth	T.S.	Description
	5160.0	Recrystallized Molluscan Packstone
5160-5161		Packstone: same above
5161-5162		Packstone: same above
5162-5163		Packstone: same above; stylolites
5163-5164		Packstone: same above
5164-5165		Packstone: same above; green waxy shale clasts, 10° dip in laminations
5165-5166		Packstone: light-gray-green to tan, medium to coarse bioclasts, moderately well sorted; recrystallized molluscan-echinoderm grains, peloids, intraclasts, oolites, superficial oolites; silt and very fine sand in matrix, glauconite; green waxy shale clasts; stylolites; laminated; infilled moldic porosity
	5166.0	Recrystallized Molluscan Packstone: faults
5166-5167		Packstone: same above; stylolites
	5166.2	Recrystallized Molluscan Packstone
	5167-5168	Packstone: same above; stylolites, 10° dip on laminations
	5168.0	Recrystallized Molluscan, Echinoderm Packstone; minor silicification
5168-5169		Packstone: same above; stylolites
5169-5170		Packstone: same above; stylolites, solution fractures infilled with calcite
	5169.7	Recrystallized Molluscan Packstone
	5170.0	Recrystallized Molluscan Packstone
5170-5171		Packstone: same above; opaques, increasing fine sand
5171-5172		Packstone: same above; solution fracture infilled with calcite, change in direction of inclination
5172-5173		Packstone: same above; stylolites, opaques, increasing fine sand
5173-5174		Packstone: same above; green waxy shale clasts prominent
	5173.1	Recrystallized Molluscan Packstone
5174-5175		Quartzarenite: light-green, very fine grained subangular to subrounded, moderately well sorted; calcareous; very silty, quartz, feldspar, glauconite prominent; recrystallized molluscan-echinoderm bioclasts, peloids, intraclasts, oolites; green waxy shale clasts, distinct laminations of bioclastic packstone; stylolites; infilled moldic porosity
5175-5176		Quartzarenite: same above

Depth	T.S.	Description
5176-5177		Quartzarenite: same above
5177-5178		Quartzarenite: same above; bioclastic packstone laminations prominent
5178-5179		Quartzarenite: same above; limestone stringers prominent
	5179.0	Recrystallized Molluscan Packstone
5179-5180		Quartzarenite: same above
5180-5181		Quartzarenite: same above; limestone stringers very prominent
5181-5182		Packstone: light-gray to green, fine- to medium-grained, moderately well sorted; sparry calcite; recrystallized molluscan-echinoderm bioclasts, intraclasts, oolites; silt and very fine sand, glauconite, green waxy shale clasts; laminated; glauconitic silt and very fine sand stringers prominent; infilled moldic porosity
	5181.1TV	Recrystallized Silty, Molluscan Packstone
	5181.2	Recrystallized Silty, Molluscan Packstone
	5182.0	Recrystallized Silty, Molluscan Packstone
5182-5183		Packstone: same above; increase in silt and very fine sand laminations, change in dip of laminations
5183-5184		Packstone: same above; stylolite, increase in silt and very fine sand
	5183.9	Recrystallized Silty, Molluscan Packstone
5184-5185		Quartzarenite: light-green, very fine grained, moderately well sorted; very calcareous; very silty, quartz, feldspar, glauconite prominent and recrystallized molluscan-echinoderm bioclasts, intraclasts, oolites; well-laminated; prominent stringers of bioclastic packstone, solution features, stylolites; infilled moldic porosity
	5185.0	Recrystallized Silty, Molluscan, Echinoderm Packstone
5185-5186		Quartzarenite: same above; opaques
5186-5187		Quartzarenite: same above; stylolites, green waxy shale clasts, limestone stringers
	5186.9	Recrystallized Molluscan, Echinoderm, Silty Packstone
	5187.0	Recrystallized Molluscan, Echinoderm, Silty Packstone: minor silicification
5187-5188		Quartzarenite: same above; limestone stringers
	5187.5	Quartzarenite: fossiliferous
5188-5189		Quartzarenite: same above; stylolites, limestone stringers prominent

Depth	T.S.	Description
	5189.0	Recrystallized Silty, Molluscan, Echinoderm Packstone
5189-5190		Quartzarenite: same above; stylolites, increase in bioclastic packstone laminations; green waxy shale clasts
5190-5191		Quartzarenite: same above; glauconite prominent, green waxy shale clasts
5191-5192		Quartzarenite: same above; stylolites, glauconite prominent
	5191.9	Recrystallized Molluscan, Echinoderm, Sandy Packstone
5192-5193		Quartzarenite: same above; stylolites
5193-5194		Quartzarenite: same above; stylolites, very little bioclastic packstone debris
	5194.0	Quartzarenite: fossiliferous
5194-5195		Quartzarenite: light-green, very fine grained subangular, well-sorted; calcareous; very silty, quartz, feldspar, glauconite prominent; minor recrystallized molluscan-echinoderm grains, oolites, intraclasts; planar laminations, distinct cross-laminations
	5194.5	Glauconitic Quartzarenite

APPENDIX B

THIN-SECTION DESCRIPTIONS

APPENDIX B

THIN-SECTION DESCRIPTIONS

The following descriptions were taken from thin sections taken from the Terra Resources, Inc., Abrahamson #1-35, NDGS Well No. 6179. Dunham's (1962) classification was used for those thin sections taken from the carbonate body. Folk's (1974) classification was used for the siliciclastics above and below the carbonate body.

Allochems, textures, and diagenetic features recognized in each thin section are listed. In many cases a bimodal grain size and roundness occurred in each thin section. These occurred with regard to the siliciclastic and bioclastic material. Grain size and roundness are given after each grouping. In cases where only minor variations occurred between thin sections, "same above" was used and the variation or addition was added to the end.

The very fine sands recognized within the packstone-grainstone facies are composed of quartz, feldspar, glauconite, and minor amounts of apatite and zircon.

Depth	Description
5020.5	Quartzarenite: quartz, feldspar, glauconite (fine- to medium-grained, subrounded), mollusk, echinoderm fragments (fine- to coarse-grained, angular); massive, bimodal grain size and roundness; poor sorting; calcareous cement, compaction, stylolites
5023.1	Quartzarenite: same above; laminated, moderate sorting
5026.4	Quartzarenite: quartz, feldspar, glauconite, opaques; fine-grained, subangular to subrounded, poorly sorted; slightly calcareous; shale lenses, bioturbated
5027.7	Quartzarenite: same above; very fine to fine-grained sands
5027.9	Quartzarenite: same above; very fine to fine-grained sands
5028.7	Quartzarenite: same above; very fine to fine-grained sands, organic partings
5031.5	Quartzarenite: quartz, glauconite, opaques, clays, very fine grained, subrounded, well-sorted; calcite cement; laminated, rippled; interparticle porosity
5031.7	Quartzarenite: same above; wavy laminations, bioturbated
5033.8	Quartzarenite: same above; massive, bioturbated
5037.0	Quartzarenite: quartz, glauconite, opaques, trace silt; very fine grained, subrounded, moderately well sorted; calcite, trace dolomite cement; massive; interparticle porosity
5041.6	Siltstone: quartz, glauconite, opaques; clays, trace very fine sand; subangular to subrounded, moderate, sorting; calcite cement; wavy laminations
5042.7	Siltstone: same above; cross-laminated, bioturbated
5043.7	Siltstone: same above; cross-laminated, bioturbated
5059.0	Mudstone: quartz, feldspar, glauconite, micaceous silts; subangular to subrounded, poorly sorted; trace calcareous cement; cross-laminated, bioturbated
5066.3	Mudstone: same above; opaques

Depth	Description
5071.1	Mudstone: same above
5074.9	Mudstone: same above
5086.3	Grainstone: mollusk, intraclasts, peloids, echinoderms, opaques, oolites; medium- to coarse-grained, well-rounded, moderately well sorted; massive; moldic porosity, silicification, dolomitization
5086.4TV	Grainstone: same above
5088.7	Grainstone: same above
5090.6	Grainstone: same above; isopachous cement
5091.3	Packstone-Grainstone: mollusk, intraclasts, opaques, peloids; medium- to coarse-grained, well-rounded, well-sorted; massive; moldic porosity, neomorphism, dolomitization
5091.4TV	Packstone-Grainstone: same above
5093.9TV	Packstone-Grainstone: same above
5093.9	Packstone-Grainstone: same above
5094.0	Packstone-Grainstone: mollusk, intraclasts, peloids, oolites, echinoderms; fine- to coarse-grained, well-rounded, moderately well sorted; massive; moldic porosity, neomorphism, trace dolomitization
5095.0	Packstone: mollusk, very fine sand (subrounded), oolites, intraclasts, peloids, opaques; medium-grained, well-rounded, poorly sorted; cross-laminated; infilled moldic porosity, fractured, stylolites
5096.7	Packstone: mollusk, intraclasts, peloids, opaques; fine- to medium-grained, well-rounded, well-sorted; massive; moldic porosity, neomorphism
5097.1	Packstone: same above
5099.0	Packstone: mollusk, peloids, intraclasts, oolites (fine-grained, well-rounded), very fine sand (subangular); bimodal grain size, moderately well sorted; massive; solution cavities, fractures, infilled moldic porosity, neomorphism, stylolites
5106.5	Packstone: same above
5109.7	Packstone: same above; finely laminated
5109.8TV	Packstone: same above; massive
5112.0	Packstone: same above; laminated
5112.4	Packstone: mollusk, intraclasts, peloids, oolites, echinoderms (medium-grained, well-rounded), trace very fine sand (subrounded); bimodal grain sizes, well-sorted; finely laminated, imbricate grains; infilled moldic porosity, minor silicification, neomorphism, recrystallization
5115.8	Packstone: same above; massive, advanced neomorphism, trace dolomitization
5115.9TV	Packstone: same above

Depth	Description
5116.3	Packstone: same above; laminations
5118.0	Packstone: same above; massive; stylolite, solution fracture
5121.6	Packstone: same above; laminated, solution fracture
5127.2	Packstone: same above; laminated, solution fractures, stylolites
5127.3	Packstone: same above; laminated
5134.4	Packstone: mollusk, intraclasts, peloids, echinoderms (medium-grained, well-rounded), very fine sands (subrounded); laminated; stylolites, infilled moldic porosity, neomorphism
5135.1	Packstone: same above; oolites
5135.4	Packstone: same above; oolites
5136.6	Packstone: same above; oolites
5138.6	Packstone: same above; trace silicification
5139.5	Packstone: same above; imbricate grains, reverse grading
5144.0	Packstone: same above; oolites; massive
5144.3	Packstone: same above; oolites; massive
5148.8	Packstone: same above; reverse grading
5153.5TV	Packstone: mollusk, intraclasts, oolites, echinoderms (medium-grained, well-rounded), very fine sand (subrounded); massive; infilled moldic porosity, solution fracture, trace silicification
5157.0	Packstone: same above; bioclasts, medium- to fine-grained, solution cavity, stylolite, trace gypsum
5159.1	Packstone: mollusk, echinoderms, intraclasts, oolites, unidentified allochem; fine-grained, well-rounded, well-sorted; massive; infilled moldic porosity, neomorphism, trace silicification, solution fracture
5160.6	Packstone: same above
5166.0	Packstone: mollusk, echinoderms, intraclasts, oolites, peloids (fine-grained, well-rounded), very fine sand (subangular to subrounded); laminated; infilled moldic porosity, stylolites, faulting, neomorphism
5166.2	Packstone: same above; imbricate grains
5168.0	Packstone: same above; trace silicification
5169.7	Packstone: same above; no faulting or stylolite
5170.0	Packstone: same above; opaques; massive
5173.1	Packstone: same above
5179.0	Packstone: same above; trace silicification
5181.1TV	Packstone: mollusk, echinoderm, oolites, intraclasts, peloids (coarse-grained, well-rounded) very fine sands (subangular to subrounded),

Depth	Description
	well-sorted; massive; trace silicification, neomorphism, infilled moldic porosity
5181.2	Packstone: same above; bioclasts (fine-grained); laminated; stylolites
5182.0	Packstone: same above; laminated, imbricate grains
5183.9	Packstone: same above; laminated, imbricate grains; reverse grading
5185.0	Packstone: same above; laminated, stylolites
5186.9	Packstone: same above
5187.0	Packstone: mollusk, echinoderm, oolites, intraclasts, peloids (fine-grained, well-rounded), very fine sands (subrounded); moderately well sorted; laminated; infilled moldic porosity, neomorphism, trace silicification
5187.5TV	Quartzarenite: quartz, feldspar, glauconite (very fine grained, sub-rounded); mollusk, oolites, intraclasts (medium-grained, well-rounded); moderately well sorted; massive; neomorphism, infilled moldic porosity, trace silicification
5189.0	Packstone: mollusk, oolites, intraclasts, peloids (fine-grained, well-rounded), very fine sand (subrounded); moderately well sorted; massive; infilled moldic porosity, neomorphism
5191.9	Packstone: same above; trace silicification
5194.0	Quartzarenite: quartz, feldspar, glauconite (very fine grained, sub-angular to subrounded), mollusk, echinoderms, oolites, intraclasts (fine-grained, well-rounded); moderate sorting; laminated; infilled moldic porosity, alteration of siliciclastics
5194.5	Quartzarenite: quartz, glauconite, feldspar, clay (very fine grained, subangular to subrounded); trace mollusk, echinoderm, oolites (medium-grained, moderate rounding), well-sorted; cross-laminated; calcareous cement; trace of altered siliciclastics